

V-1

OLIVINE ABUNDANCES AND COMPOSITIONS IN HAWAIIAN LAVAS

By

J. Brian Balta

Michael B. Baker

Edward M. Stolper

ABSTRACT

Crystallization of olivine phenocrysts is the dominant differentiation mechanism of Hawaiian lavas. Some fraction of these olivine crystals are entrained within liquids as they erupt and produce the typical whole rock compositions of Hawaiian lavas that lie on mixing trends between basaltic liquids and olivines. Understanding the relationship between the olivines and the liquids that host them is key to interpreting data obtained on whole rocks, glasses, and mineral separates. The continually increasing supply of whole rock and olivine compositional analyses from Hawaiian volcanoes and the new availability of large, stratigraphically-controlled data sets from the Hawaii Scientific Drilling Project (HSDP) has allowed us to undertake a detailed analysis of the mixing process between Hawaiian basalts and crystallized olivines. The HSDP drill cores suggest that there is significant variability in the quantity of olivine carried by liquids through time, possibly related to changes that occur during volcanic evolution. We use these data sets to calculate estimated equilibrium parental liquid compositions for the best-sampled Hawaiian volcanoes and to test whether the olivine addition calculations are consistent with the bulk rock sample analyses.

1. INTRODUCTION

Over the past few years, sampling and analysis of the compositions of whole rocks and minerals making up the Hawaiian Islands has produced a wealth of new data that allows for the application of statistical techniques and chronological analysis of the growth and evolution of Hawaii at scales that were previously not practical. The Hawaii Scientific Drilling Project pilot hole (hereafter HSDP1) produced 1056 meters of core sampling 27 distinct lithologic units from Mauna Loa and 184 units from Mauna Kea (DePaolo et al., 1996). The second HSDP core (hereafter HSDP2) produced 3098 meters of core, sampling 32 units from Mauna Loa and over 300 units from Mauna Kea, including 2019 meters of submarine material and covering nearly 650 k.y. of time (Garcia et al., 2007). While the HSDP cores provide the most complete stratigraphic and chronological data set available for any Hawaiian volcano, other coring and sampling efforts have provided data covering many other Hawaiian volcanoes. The Ko'olau Scientific Drilling project (hereafter KSDP) produced 679 meters of core from Ko'olau volcano on the island of Oahu, sampling 103 units from that volcano (Haskins and Garcia, 2004). The SOH-1 drill core produced ~1700 meters of core from Kilauea's East Rift Zone, sampling 368 units (Quane et al., 2000). Drill cores are also not the only sampling technique that has produced a large quantity of data from Hawaiian volcanoes. The long-lived Pu'u O'o eruption of Kilauea has been monitored and sampled in great detail (e.g., Thornber et al., 2003). Offshore sampling efforts have produced representative data from many of the volcanoes in the Hawaiian chain, and many of these samples have been dateable due to associated biological activity (e.g., Clague et al.,

1995). The work of Sobolev et al., (2007) produced a large number of analyses of olivine compositions from several Hawaiian volcanoes, in addition to other studies of the same mineral (e.g., Helz, 1987; Garcia, 1996). Finally, onshore sampling of exposures and eruptions continues to improve the data available covering many of the Hawaiian shields (e.g., Rhodes, 1988; Marske et al., 2007).

Changing conditions during the growth of a volcano, such as changes in magma supply or average liquid composition, can affect the composition of the eruption products. Measurements of the compositions of erupted liquids and solids can give information on these changes and on the conditions under which they formed. Highly forsteritic olivines, with Mg #'s ($= 100 * X_{Mg} / (X_{Mg} + X_{Fe})$ on a molar basis) of 90 or above are found in Hawaiian lavas, and olivines with slightly lower Mg # are common, indicating that Hawaiian basalts must begin their fractionation process as highly magnesian liquids (e.g., Clague et al., 1991; Clague et al., 1995; and Garcia et al., 1996). However, analyses of the lavas being erupted from Hawaiian volcanoes indicate that very few lavas and no glasses have high enough MgO contents and MgO/FeO ratios to be in equilibrium with such primitive olivines. These facts suggest that some fraction of the olivine that crystallizes from the parental liquid is never erupted and is deposited within the volcanic plumbing system. (e.g., Clague and Delinger, 1994; Rhodes and Vollinger, 2004).

It has long been established that olivine-control lines define the main compositional variations amongst Hawaiian shield-stage lavas (e.g., Wright, 1971). The process generating this variation in Hawaiian lavas is now fairly well understood; highly

magnesian parental magmas rise through the crust, stall at a level of neutral buoyancy, and begin to crystallize olivine as they cool (e.g., Ryan, 1988; Garcia and Wolfe, 1988). Variable amounts of the crystallized olivine are entrained by erupting liquids as they move upwards, while other crystals are left behind within the volcano and form a dense, olivine-rich cumulate pile within the volcano (e.g., Clague and Denlinger, 1994; Kauahikaua et al., 2000). This description is a simplification as it is complicated by the effect of volatiles, which can decrease the overall density and therefore drive eruptions (e.g., Anderson, 1995), and entry of new magma into the system, which can displace earlier liquids from the magma chamber (e.g., Garcia, 1989). The mixing behavior that generates olivine abundance variations in a magma was demonstrated on a smaller scale by the 1959 Kilauea Iki eruption, which was originally erupted as a moderately olivine-phyric lava in a fire-fountaining event driven by volatile degassing (e.g., Gerlach and Graeber 1985; Decker 1987) but also formed a lava lake that slowly crystallized and mixed. This combination of crystallization and mixing created whole rocks that vary from highly olivine phyric to nearly aphyric due to addition and subtraction of olivine (Richter and Moore, 1966). A similar process likely works to generate heterogeneity in bulk rock olivine contents on a magma-chamber scale. As this process is evidently common in Hawaiian volcanoes, a more thorough examination of the processes leading to variable amounts of olivine within and between the Hawaiian shields should provide insight into the development of those volcanoes.

Clague and Denlinger (1994) calculated that based on their estimated parental magma for Kilauea, between 10 and 22% of the original mass of magma entering the

volcano remains within the volcanic edifice as olivine cumulates. The common occurrence of dunite xenoliths (e.g., Jackson, 1968), along with the evidence for a high-density anomaly near the core of each volcano (Kauahikaua et al. 2000), suggests that the missing olivine is deposited inside the volcano as the magma stalls and crystallizes. Conversely, the common occurrence of strained olivine grains within Hawaiian lavas suggests that olivines can be re-entrained in magmas as they move through the system (e.g., Helz, 1987), as those olivines must have resided for a time in a partially solid pile that is able to transmit shear stresses. Based on the HSDP1 drill core, Baker et al. (1996) estimated that only 4% of the mass of magma entering Mauna Kea is deposited as olivine within that volcano. Understanding the processes by which olivine grains are processed prior to eruption is particularly important for geochemical analyses, as mineral separates are often used to analyze isotopic compositions of Hawaiian rocks, and a close relationship between olivine grains and their host melt is a standard assumption in those analyses.

This paper will use the newly available databases covering a number of Hawaiian volcanoes including Mauna Kea, Mauna Loa, Kilauea, Hualalai, Loihi, and Ko'olau, to examine in detail the relationship between olivines and the melts that host them. We estimate the amount of olivine being stored within each volcano, and the bulk compositions of olivine that fractionate as the parental liquids evolve to liquids that represent the groundmass of erupted lavas, and calculate the parental magma compositions feeding the Hawaiian system.

2. METHODS

2. 1. Data compilation

Over 6700 whole rock analyses of Hawaiian basalts, 1700 glass compositions, and 8200 olivine analyses (including the data from Sobolev et al., 2007) were compiled from the literature and the GEOROC database (<http://georoc.mpch-mainz.gwdg.de>) (Sarbas and Nohl, 2008); data. Sources for this database are listed in Supplementary Table 1.

Whole rock analyses were processed as follows. Iron analyses were recalculated with all iron taken as FeO*. Data were sorted first by volcano and then filtered to produce data sets for each volcano where the variation is dominated by mixing of tholeiitic basalt (with 7-8% MgO) with olivine. First, all samples with less than 7 wt % MgO were eliminated to avoid samples that had crystallized significant amounts of phases other than olivine, which typically reach saturation at ~7% MgO (e.g., Richter and Moore, 1968; Wright and Peck, 1978). However, it is also possible that a liquid could fractionate to below this MgO content and then re-entrain enough olivine to produce a whole rock composition that meets this standard. For volcanoes such as Kilauea, Mauna Loa, or Mauna Kea, where there is a large amount of data available, making this filter more selective by limiting the dataset to samples above 7.5% MgO does not significantly change any of our conclusions and typically only removes a small number of samples, suggesting that the effects of plagioclase and clinopyroxene fractionation on rocks not removed by this filter is limited. The second filter applied to the data sets used the K₂O/P₂O₅ ratio to screen for samples that were highly altered. We removed all samples with K₂O/P₂O₅ ratios greater than 2.0 (Huang et al., 2007) or less than 1.0 (Huang and Frey, 2003). Again, a more stringent filter, removing all samples with K₂O/P₂O₅ less than

1.4 was tested and found to have no significant change on our conclusions. Finally, we filtered out all points that were from alkaline rocks, using the definition of alkali index from Rhodes and Vollinger, (2004). These filtering steps excluded over 50% of the whole rock analyses available for Hawaii, although some volcanoes were more heavily filtered than others (Table 1). Data sets built from the analyses passing these successive filters form the basis of the regression analysis presented here.

2. 2. Conversion between mineralogy and geochemical analyses

For samples from the four major drill cores examined by this study, along with various other data sets, published point counting results are available for modal olivine abundances. To supplement the existing data in Garcia et al. (2007), we conducted a series of 43 point counts on slides from the Caltech Reference Suite of samples from the HSDP2 drill core (Table 2). Between 500 and 800 points were counted and identified as olivine, vesicles, plagioclase, or matrix. Phases <0.5 mm were considered part of the groundmass, similar to the standard used by Baker et al. (1996). The typical step size was 1 mm. One sample was counted on four separate occasions to yield an estimate of the uncertainties on the mode, which were found to be $\pm 2\%$ absolute olivine abundance. The abundance of olivine, which has MgO content near 50 wt. %, should be strongly correlated with the whole rock wt. % MgO. There is expected to be some scatter, as the sample used to make the thin section may not always be fully representative of the larger sample used for bulk rock analysis. In general, each volcano shows a linear relationship between modal olivine and whole rock wt. % MgO (Figure 1). We derived a regression line for each volcano, as was done by Baker et al. (1996). Essentially all of the slopes of

the different regression lines overlap at the 1σ level. There is some scatter around each line, although this is typically less than 10 % absolute olivine modal abundance (1σ). Each of the data sets from the different volcanoes overlaps at the 1σ level, suggesting that modal olivine abundance can be estimated with good precision for any Hawaiian sample from the whole rock MgO content. In this database and in Fig. 1, this variation in modal olivine at a constant MgO content provides an estimate of the variation inherent in analyzing samples of variable size from different portions of units with possible variations in liquid compositions superimposed. This comparison suggests the variation seen here is the magnitude that should be expected in any work based on point counting from similar rock types.

A key issue for the data presented in Figure 1 is the handling of vesicle contents. As whole rock analyses use crushed or fused rock powders, the vesicle content in a sample will have no effect on the whole rock composition. However, volume percentages measured via point count can be sensitive to the percentage of vesicle space in a given thin section. In Figure 1, the olivine volume percentages were normalized to total vesicle-free volume in the point count. This correction can potentially be a source of significant error (and hence a source of scatter in Figure 1) as the variation in vesicle contents can be large even within individual flows (Self et al. 1998). To minimize this issue, we adopt for all unknown samples the linear relationship between whole rock wt. % MgO and olivine contents defined by regression of the point counts from HSDP2 normalized to vesicle-free volume for any sample with a whole rock analysis but no available point counts. We

will generally present data as whole rock weight % MgO, but conversion to olivine abundance can be done simply with the expression from Figure 1.

2. 3. Chronology

Determining approximate ages for units in the available drill cores is a necessary step in understanding the evolution of these magmatic systems over time. For HSDP1 and HSDP2, we adopt the age versus depth relationships of Sharp and Renne, (2005), based on ^{40}Ar - ^{39}Ar dating performed on the HSDP2 drill core.

Ages in the other drill cores are less well constrained. The SOH-1 drill core, and its companion hole SOH-4, have been dated by ^{40}Ar - ^{39}Ar and produced ages ranging up to 350 ka for the oldest rocks (Quane et al., 2000). However, other dating has suggested that the Kilauea pre-shield stage may not have ended until 130 ka (Lipman et al., 2000). Teanby et al. (2002) performed a detailed paleomagnetic survey of the subaerial portion of the SOH-1 drill core and could not reconcile the radiometric ages with paleomagnetic age estimates. They calculated an age progression that dated the bottom of the subaerial portion of this drill core at 45 ka, giving an accumulation rate of just over 15 m/k.y. for that section of the core. This rate is consistent within a factor of two with the accumulation rates estimated by Sharp and Renne (2005) for Mauna Kea and is well-fit by the growth model for Hawaiian volcanoes of Depaolo and Stolper (1996). Assuming that this average accumulation rate persisted over the submarine section of the SOH-1 drill core gives an age of 107 ka for the bottom of the core. We therefore used the age model of Teanby et al. (2002) for the subaerial section and this constant accumulation rate for the submarine section of this core.

Applying an appropriate age model to the KSDP drill core also is difficult. Several ^{40}Ar - ^{39}Ar dates were reported by Haskins and Garcia (2004), but given the age of the rocks and the uncertainty in the measurements the ages of the top and bottom of the drill core were indistinguishable. Based on the data from the other drill cores, however, a reasonable chronology for the KSDP sequence can be constructed. The reported errors in ages from Haskins and Garcia (2004) were ± 200 k.y. An average accumulation rate at the KSDP site of 3 m/k.y. or less would mean that the KSDP core would represent more than 200 k.y. of time and should have yielded ages that were measurably distinct, placing a lower bound on the accumulation rate. Placing an upper bound on the accumulation rate at this site is more difficult, but the KSDP core samples material from the latter stages of activity of Ko'olau when the volcanic activity was presumably waning. An average accumulation rate of 5 m/k.y. at the site gives a total age of just over 100 k.y. for the flows reflected in the core and a resurfacing interval of 1000 years for the site, similar to that reported for Mauna Kea (Garcia et al., 2007), so this is the accumulation rate we have chosen as an average for this core. However, we have no ability to recognize changes in accumulation rate and may be missing events such as a change in accumulation rate with time like that seen in Mauna Kea.

3. RESULTS

3.1 Olivine regression analysis

There are sufficient bulk rock analyses for eight Hawaiian volcanoes to construct statistically meaningful olivine control lines in the sense that when extrapolated to the olivine composition line, the olivine composition is constrained within ± 1.2 Mg#. These

include: Kilauea, Ko'olau, Haleakala, Mauna Loa, Mauna Kea, Loihi, Waianae, and Hualalai. The full set of bulk rock analyses and olivine control lines are shown in Figure 2. Each volcano is well fit by an olivine control line calculated via unweighted least squares linear regression. The differences in slopes reflect differences in the liquid compositions at each volcano that entrains olivine and differences in the average composition of the entrained olivine.

Projecting the linear regression lines in these analyses from the available data set towards the composition line representing an olivine end member (including minor and trace components as calculated in the olivine addition analysis below) allows for determination of the average olivine composition mixing in each volcano's magma series, as was done with a more limited data set from HSDP1 in Baker et al. (1996). With these data sets, several differences become apparent. Most notably, there appear to be some volcanoes which have different average olivines at the end of their olivine control line trend. Mauna Kea, Hualalai, and Mauna Loa appear to contain on average more forsteritic olivines, with Mauna Kea averaging Mg# 87.9, Hualalai averaging Mg# 87.4, and Mauna Loa averaging Mg# 87.3. Conversely, Ko'olau, Waianae, and to a lesser extent Kilauea sample olivines that are slightly more fayalitic than olivines from other volcanoes, with Ko'olau averaging Mg #86.2 and Kilauea averaging Mg# 86.6. Loihi, and Haleakala sit in-between these volcanoes and are indistinguishable from each other.

The differences in these data sets can be visualized from Figure 2 by noticing the differences in slope and absolute FeO* content of the regression lines at 7 wt% MgO between the volcanoes. Mauna Kea has a noticeably flatter slope to its olivine control line

compared to the other volcanoes, which reflects the higher Mg # of the olivine in its whole rocks, while Ko'olau and Waianae show slopes that are somewhat steeper than those of the other volcanoes. The differences in FeO* between volcanoes are small and most of the volcanoes are statistically indistinguishable (Figure 3). Ko'olau and Mauna Kea appear to be the only two volcanoes with FeO* contents that can be distinguished. At 7% MgO, Mauna Kea averages $\text{FeO}^* = 11.3 \pm 0.4$, while Ko'olau averages $\text{FeO}^* = 10.4 \pm 0.3$. The other volcanoes all fall within the range of FeO* 10.5-11.0, except for Loihi, which averages $12.0\% \pm 0.5$ but is less well sampled than the others. In Figure 3 we plot histograms of olivine abundance for Mauna Kea and Ko'olau to illustrate the different average FeO* contents. Notably, Ko'olau shows a larger range in FeO*, and many of its higher FeO* content samples are also more olivine-phyric, suggesting that the small difference in FeO* may be entirely due to the different average olivine composition being crystallized from the volcano. Loihi may actually show higher FeO* contents across its full range of samples, but more sampling is required to better constrain the variability at the low-olivine end.

We also applied a similar regression analysis to the available drill cores. All of the drill core data are included in Figure 2, but only for Mauna Kea do they constitute 50% or more of the available whole rock analyses. The SOH-1 core through Kilauea was not useful for olivine control regression analysis as there were not enough olivine-rich points to generate a significant trend. The HSDP cores through Mauna Kea and Mauna Loa and the KSDP core through Ko'olau all produce trends that cannot be distinguished within error from the trends seen in the full data sets from the same volcano, suggesting that the

full data sets are representative of the behavior of the volcanoes over time. Mauna Kea's average olivine composition as predicted by the bulk rock HSDP2 FeO*-MgO regression is indistinguishable from that reported by Baker et al. (1996) for the HSDP1 core, which sampled only subaerial Mauna Kea flows. Stolper et al. (2004) identified two different magma series in the HSDP2 glasses from Mauna Kea defined by high and low silica compositions. Using their definition for high and low silica glasses and taking whole rock analyses from the same units, we have sufficient data to define olivine control line trends for both magma series. Both high and low SiO₂ units mix towards olivines with Mg # of 87.9, again indistinguishable from the full core (Figure 4).

For volcanoes where >100 olivine composition measurements are available, the measured olivine compositions provide an alternate way to infer the composition of the average added olivine. Six volcanoes have a sufficient number of reported olivine compositions to allow for an analysis of their populations (Figure 5). We plotted histograms of individual analyses from these volcanoes, most of which sample the composition of the core of a single grain. The distributions for several volcanoes show sharp peaks around Mg# 88, while Hualalai and Ko'lau show more broad patterns. Mauna Loa shows on average the most magnesian olivine, with a median value of Mg# 88.9, followed by Mauna Kea at Mg# 87.9, which is the exact value calculated from the olivine control line. The mean absolute deviation for these two volcanoes is 2.0 units. Mauna Loa shows a median value with a slightly higher Mg# than its average composition seen in the regression analyses, but the values overlap within error. This slight difference could occur if the olivines selected for analyses were slightly biased

towards higher Mg# olivines, such that the distribution of analyses is not fully representative of the mass distribution of olivine compositions. Ko'olau and Loihi both have a median average olivine measured at Mg# 86.6, again similar to the olivine control line trend. The mean absolute deviation for both is also constrained to better than 2 units. Hualalai and Ko'olau each show evidence of two separate abundance peaks, one close to Mg# 88 and another close to Mg# 84. Several authors (e.g., Clague, 1988; Shamberger and Hammer, 2006) have argued that the dunites from Ko'olau and Hualalai represented the products of crystallization from post-shield, alkali magmas. This lower peak at Mg# =83-84 appears in Ko'olau, Mauna Kea, and Hualalai, and according to our data set most of these samples represent olivines from post-shield magmatism or dunites. The peak in Mauna Kea is small compared to the other volcanoes because many of its measured olivines come from the HSDP drill cores, which sample much of its shield-building stage. Kilauea also shows a large peak at Mg# 88, but also has significant quantities of olivine with Mg#'s below those measured from any other volcano. The large spread of olivine compositions for Kilauea also increases the mean absolute deviation to 4.1 units in Mg#. These low-Mg# olivines from Kilauea typically represent the products of crystallization of magmas that evolve in the magma chamber (e.g., Garcia et al., 1989) or the product of re-equilibration inside lava lakes (Moore and Evans, 1967). While these processes likely occur at all Hawaiian volcanoes, these low Mg# olivines may be found most commonly in Kilauea because of the detailed sampling done during the full duration of eruptions, whereas other volcanoes are sampled more commonly as individual events long after deposition. In these cases, the earliest or latest olivines in an eruption may be less likely

to be sampled and thus are only seen in substantial quantities in Kilauea. Except for Kilauea and Hualalai as noted, the average and median compositions for all the volcanoes calculated in this analysis overlap within error of the average olivine composition calculated by the olivine control line regression analysis.

3.2. Olivine abundance chronology

The chronologic series of units in HSDP2 and the other drill cores was analyzed for olivine abundances over time, as represented by the bulk MgO content of the rocks (Figure 6). Using the bulk rock analyses, the thicknesses of the measured units, and point count data including the average vesicle content of the units where available, we have calculated a bulk average composition of the volcanoes sampled by the HSDP1, HSDP2, KSDP, and SOH-1 drill cores. These bulk average compositions are given in Table 4d. To perform this calculation, we averaged the bulk composition analyses for each drill core weighted by the thickness of each unit on a vesicle-free basis. This exercise was hampered by the fact that not all of the units in each drill core were sampled by both point counts and bulk rock analyses. In addition, we could not correct the KSDP drill core thicknesses for vesicle count as the vesicle abundances were not explicitly recorded, so the raw thicknesses were used (Haskins and Garcia, 2004). Both Mauna Loa and Mauna Kea in the HSDP sections are highly olivine-phyric compared to the KSDP and SOH-1 drill cores. On average, the HSDP2 Mauna Loa section contains 13.6% MgO, Mauna Kea's HSDP2 section contains 14.1% MgO, the KSDP section contains 8.5% MgO, and the SOH-1 section contains 7.6% MgO. Based on the calibration given in Figure 1, these equal 16.4 volume % olivine for Mauna Loa, 15.6 volume % olivine for

Mauna Kea, 3.3 volume % olivine for Ko'olau, and 1.4 volume % olivine for Kilauea. This value for Mauna Kea is similar to the integrated MgO abundance of 13.2% calculated by Baker et al. (1996) for the Mauna Kea section of the HSDP1 drill core. However, the value for the SOH-1 drill core is less than the average MgO abundance for either bulk Kilauea (10 wt.%) or for only subaerial Kilauea flows (9 wt.%) estimated by Clague and Denlinger (1994). Clague and Denlinger (1994) based their estimate in part on individual samples collected from specific eruptions, without correction for the volume of erupted material or long-term sampling, which may explain the difference in estimated bulk Kilauea composition.

There is a difference in sampling density between the cores that could provide a substantial margin of error to this examination if units are not sampled at random. The geochemical analyses of the KSDP drill core samples represent over 90% of the total thickness of units, the HSDP2 drill core samples represent approximately 75% of the total thickness of units (depending on how individual intrusive units are counted), while the SOH-1 analyses only sample approximately 33% of the total thickness of units.

The HSDP2 core through Mauna Kea produces a detailed record of the variations in olivine deposition at the drill site through much of the growth of the volcano, while the other drill cores provide samples of specific intervals of the lifetimes of those volcanoes. Several differences can be seen by comparison of these cores (Figure 6). First, the SOH-1 core through Kilauea has lower olivine content than any of the other Hawaiian volcanoes sampled. Secondly, the latter stages of each volcano's lifetime, represented by the flows through Mauna Loa in HSDP2 (e.g., Moore and Clague, 1992; DePaolo and Stolper,

1996), the KSDP core through Ko'olau (Haskins and Garcia, 2004), and the latter part of Mauna Kea's lifetime in HSDP2 (Sharp and Renne, 2005), is marked by high-frequency variation in the olivine content being deposited at these drill sites, with swings from low to high average olivine contents on about a 20 k.y. timescale. This behavior can be seen in the sequences for Mauna Loa, Ko'olau, and in the portion of Mauna Kea younger than 420 ka, and is well expressed in the changes in the calculated moving averages with depth (Figure 6). Younger than 330 k.y., Mauna Kea again shows limited variation but also shows more sparse sampling, mostly within its postshield lavas. Conversely, the SOH-1 core and the majority of the submarine section of the HSDP2 core show fairly stable trends in olivine abundance with time; the average olivine contents only change on timescales of 100 k.y. The lowest portion of the HSDP2 core, however, again shows more rapid changes in olivine content.

Although not plotted here, the HSDP1 section through Mauna Loa and Mauna Kea shows similar behavior to the upper portion of HSDP2 in both the high-frequency variation in olivine abundances and in the olivine-controlled bulk composition, measured to be 13.2% MgO (12.5% olivine) on average in Mauna Kea in HSDP1 (Baker et al., 1996) and 13.9% MgO (14% olivine) for the subaerial section of Mauna Kea in HSDP2. Conversely, the deeper portion of Mauna Kea and the section through Kilauea shows a different style of behavior, with longer periods of steady olivine contents.

The pattern of MgO abundances in Mauna Kea changes immediately below the submarine to subaerial transition at a calculated age of 413 ka. The upper submarine deposits are highly olivine-phyric, and the abundance of olivine gradually decreases with

increasing depth. The moving average of whole rock MgO shown in Figure 6 reaches a local maximum of 20.07% MgO (26.8% olivine) at 444 ka and decreases steadily deeper in the section to a local minimum of 10.25% MgO (6.4% olivine) at 584 ka. The 67 k.y. section just below the subaerial/submarine transition averages 17.42% whole rock MgO (21.3% olivine). The lower portion of this trend, covering a period of nearly 80 k.y. from 530 k.a. to 610 k.a., averages only 11.45% MgO (8.9% olivine). This is a much lower olivine content than has been measured for any extended portion of Mauna Kea in this area prior to sampling in HSDP2. This trend continues across different flow unit types and across both the low and high SiO₂ magma series. The bottom section of the core seems to resume more high-frequency variation, but this appears to be due to the presence of a series of high-olivine pillow basalts. Aside from these deep pillows, the trend of decreasing olivine abundance includes both hyaloclastite and massive units and even some pillow lavas (Figure 6).

3.3. Historic flows

The modern magmatic activity provides a final set of data to allow for comparison between the olivine abundances in the drill cores and the full magmatic history. Analyses of the available, well-dated historic flows for Mauna Loa and Kilauea are plotted in Figure 7. Both volcanoes show significant variation in olivine content between and within successive flows, some of which can be related to crystallization and accumulation within a particular unit. The modern Kilauea flows prior to 1983 average 8.30 wt. % MgO, with no weighting by unit thickness, volume, or number of samples per unit; a number similar to the low whole rock MgO value seen in the SOH-1 drill core.

The modern Mauna Loa flows, similarly unweighted, average 9.11 wt. % MgO, greater than seen in modern Kilauea flows but significantly less than the average seen for Mauna Loa flows in the HSDP drill cores. For future flows, including the current Pu'u O'o eruption at Kilauea, accurate estimates of the volume of extruded material will make these analyses far more complete.

The modern eruption of Pu'u O'o currently consists of 3.38 cubic kilometers of material, up to 35 meters thick, according to data published by the Hawaiian Volcano Observatory (see http://hvo.wr.usgs.gov/kilauea/summary/Current_table.html). This thickness is comparable to some of the larger units sampled in the HSDP cores, which are tens of meters to roughly one hundred meters in thickness. The Pu'u O'o eruption has been sampled in great detail, and therefore provides an example for the evolution of olivine abundances during a single eruption (Figure 8). The average whole rock MgO in the Pu'u O'o eruption is 8.19 wt. % (2.1% olivine), similar to the long-term average composition for Kilauea and to the bulk average seen in the SOH-1 drill core. Samples from the Pu'u O'o eruption do show some variation in olivine abundance, reflected by the whole rock wt. % MgO analyses in Figure 8. The variation in olivine abundance in the Pu'u O'o eruption is less in magnitude than the variation seen in Figure 1 (~3% olivine abundance), suggesting that intra-unit variation can make up a small part of the scatter seen in that figure.

3.4. Olivine addition calculations

The average basaltic liquid erupted by Hawaiian volcanoes contains 6-8 wt. % MgO (e.g., Wright and Fiske, 1971; Thornber et al., 2003; Stolper et al., 2004). A

significant amount of olivine must crystallize to move a melt from equilibrium with olivines with Mg # of 90-91 to those typical liquid MgO contents (e.g., Basaltic Volcanism Study Project 1981; Clague et al., 1995; Baker et al., 1996). Starting from typical glass compositions for the best-studied Hawaiian volcanoes, we have mathematically reversed this process to calculate the liquids that would be in equilibrium with the most highly magnesian olivine sampled in each volcano. Average glass compositions were obtained for the best-sampled volcanoes in Hawaii: Mauna Kea, Mauna Loa, Kilauea, Ko'olau, and Hualalai (Table 4) to use as starting points. The initial starting glasses for the calculation were calculated by averaging glass measurements with >7% MgO to ensure that the starting liquids were only saturated with olivine and spinel. The calculations were performed by adding 0.1 % of equilibrium olivine to the glass or whole rock composition at each step. For completeness, at every step we also added 0.001% of a chromian spinel, based on the ratio given in Roeder et al. (2006). The spinel added was an average spinel composition from Pu'u O'o as measured by Roeder et al. (2003).

The olivine-melt Fe-Mg exchange parameter K_D is the key variable in these calculations. Calculations were performed first with the olivine K_D parameterized following the method of Toplis (2005). For that parameterization, we chose values of H₂O content to be 0.7 wt % (similar to average H₂O content of undegassed samples from Seaman et al. (2004)), a pressure of 1 bar, and a temperature at each step calculated using the olivine-liquid thermometer of Beattie (1993). This leads to some variation in calculated K_D values between the volcanoes due to the differing initial compositions; the

lowest average K_D was .305 in the Mauna Kea low SiO₂ series, and the highest was .318 at Haleakala. An oxygen fugacity of 1 unit below the quartz-fayalite-magnetite buffer was assumed based on recent analyses of olivine-melt equilibria (e.g., McCann and Barton, 2005), and Fe²⁺/Fe³⁺ ratios were calculated at this oxygen fugacity using the calibration of Kilinc et al. (1983). Nickel and manganese were considered in the olivine and calculated based on the experimentally calibrated expressions of Wang and Gaetani (2008). Nickel contents were typically not measured in glasses, and so a value of 0.008% was used as the initial glass starting composition; this produced high-Mg# olivines containing ~0.5% NiO, similar to values measured by Sobolev et al. (2007). Calcium, chromium, and aluminum were included in olivine in small proportions based on average olivine compositions from Hawaii from the GEOROC database and assuming charge-balancing for the +3 oxidation state cations by putting ½ the Cr and Al in the tetrahedral site and ½ in the octahedral site.

The olivine addition calculations continued until the calculated olivine was equal to the most magnesian olivine reported in the GEOROC database for each volcano. Mauna Loa and Hualalai show olivines up to Mg# 91.2, Mauna Kea shows one sample in the Sobolev et al. (2007) database with Mg# 91, but the remainder of its olivines are 90.5 and below and this analysis appears uniquely high. The highest recorded Mg# olivine for Kilauea is 90.7. For Ko'olau, most of the existing analyses come from xenoliths or from post-erosional flows. A few samples have Mg # greater than 91, but the highest Mg # in a lava flow was 90.5 recorded in a basanite (Sobolev and Nikogosian, 1994), and this olivine was used as the stopping point for the olivine addition in that volcano. For

Haleakala there are available glass compositions but not extensive analyses of olivine compositions, and so we assumed its olivines were similar to Ko'olau and Mauna Kea. A few very highly forsteritic olivines (up to $Mg\#=97$) have been found in Hawaii, but Garcia et al. (2000) noted that these are likely alteration products created by high-temperature alteration producing magnetite and hypersthene by replacing the original olivine, and thus they will not be considered here.

The variety of data sets available in this analysis gives us a new ability to assess the utility of these calculations. Because we know the mass of olivine added in each step and its composition, it is trivial to calculate the average olivine composition added. This number can then be compared with the average olivine compositions seen in the previous analyses. For most of the volcanoes considered here, the match between the average added olivine and the olivine composition inferred from the olivine control line in FeO^*-MgO space is quite good (Table 4). The olivine addition calculation predicts that the average olivine in Mauna Loa ($Mg\# = 87.7$) and Hualalai ($Mg\# = 87.5$) is more magnesian than that found in Ko'olau ($Mg\#= 86.5$), Kilauea ($Mg\# = 86.7$), and Haleakala ($Mg\# = 86.7$), and all of these calculated average olivine compositions lie within the errors of the mean values seen in the regression analysis or the mean absolute deviation of the histogram populations. Because the olivine compositions added to Ko'olau are calculated to be slightly different than the olivine compositions added to the other volcanoes, the difference in whole rock FeO^* contents from Ko'olau shown in Figure 3 disappears as the calculation proceeds, suggesting that the slightly low FeO^* contents in Ko'olau are a consequence of the composition of olivine being crystallized.

Mauna Kea, notably, shows a mismatch between the average added olivine composition and the olivine control line and histogram trends; the average added olivine is less forsteritic than seen in the other analyses. Mauna Kea's olivine addition trends produce average olivines of Mg# 86.4 and 86.7 for the high and low SiO₂ series, respectively, compared to Mg# = 87.9 in the regression analysis. There are a number of possible explanations for this result, which we consider below. It is possible we are underestimating the final olivine Mg# at which we should end the calculation by stopping at Mg# 90.5. If we extend the calculation to Mg# 91 to match the single olivine from Sobolev et al. (2007), it improves the match but does not entirely resolve the discrepancy (average added Mg# = 87.2 and 86.9), and also increases the MgO content of the calculated liquid substantially. An alternate possibility is that Mauna Kea is actually producing less low-Mg# olivine. One method by which this could be achieved is a rapid flushing of new magma through its system sustained by a very high magma flux; in this case, the average liquid in the magma chamber would remain above 7% MgO and olivines with lower Mg#'s would not be involved in the mixing process in the magma chamber. By rapidly flushing the magma through Mauna Kea, the low-Mg# olivines we assume in our calculation would only have crystallized after eruption, if at all. A similar suggestion was offered by Rhodes and Vollinger (2004) as an explanation for the lack of low-MgO content whole rocks over a substantial portion of the HSDP2 drill core. We tested this suggestion in the olivine addition calculation by using starting glass compositions created by averaging only glasses from Stolper et al. (2004) with >8% MgO. In this case, we were able to produce a much better fit to the expected average

olivine composition ($Mg\# = 88.0$ and 87.7). If we start the olivine addition calculation with a liquid at $\sim 9\%$ MgO, we can produce an adequate fit to the average olivine composition with a parental liquid consisting of the liquids given in Table 4b with 17% MgO and with a maximum olivine $Mg\#$ of 90.5, suggesting that 9% MgO is the highest MgO content of the erupting liquid that would be consistent with the olivine addition trends.

3.5 Olivine CaO contents and re-equilibration

To better understand the applicability of these olivine control lines and olivine addition calculations to the evolution of natural Hawaiian magmas, we also examined the CaO compositions of olivines for the sampled volcanoes (Figure 9). CaO was ideal for this analysis, since we have both high-precision analyses of olivine CaO contents and a calibration for the variation of CaO in olivine during crystallization (e.g., Libourel, 1999). In addition, the diffusion rates for CaO in olivine are slower than for MgO or FeO (Jurewicz and Watson, 1998b) and thus CaO can preserve information that other oxides do not. For this analysis, we focused on the olivine composition measurements from Sobolev et al. (2007) because in this single data set we know that all analyses were obtained under the same analytical conditions and with appropriate settings to analyze low-concentration elements with minimal errors. This limited us to the five volcanoes sampled in that study; Loihi, Mauna Kea, Mauna Loa, Ko'olau, and the Kilauea Iki eruption from Kilauea.

Libourel (1999) developed an empirical model for CaO partitioning between olivine and melt that allowed for estimation of the CaO content of olivine in equilibrium

with silicate melts. That model predicted that as a Hawaiian magma evolves from crystallizing olivines with Mg# 90 to Mg# 80, there should be a substantial increase in the CaO content of the olivine (the red line shown in the panel for Mauna Kea in Figure 9) from ~0.2% to ~0.4% due to increasing CaO contents in the melt and increasing D_{CaO} (=CaO concentration in olivine/CaO concentration in liquid). After the liquid reaches ~7% MgO and begins to crystallize olivine with Mg# ~ 81, the liquid reaches plagioclase saturation and the CaO content of the olivine should then begin to decrease because of decreasing liquid CaO contents (e.g., Wright and Peck, 1978; Libourel, 1999). The available Hawaiian olivine analyses show a more complicated pattern (Figure 9). Every volcano shows low CaO contents of ~ 0.2% in their highly magnesian olivines, consistent with the prediction of Libourel (1999). However, as crystallization proceeds, the patterns diverge. Ko'olau and the olivines from Kilauea Iki show fairly flat trends, with less increase in olivine CaO content than predicted by the model of Libourel (1999). Mauna Kea and Loihi show some olivines that increase in CaO content with decreasing Mg# as predicted by Libourel (1999), but also have an additional population that varies between this trend and the nearly-flat trend similar to Kilauea and Ko'olau. Finally, Mauna Loa shows most of its olivines along a flat trend, similar to Kilauea and Ko'olau, but has a small group of olivines that show elevated CaO contents, similar to the high CaO olivines from Mauna Kea and Loihi but fewer in number.

The increasing CaO content in olivine predicted by Libourel (1999) occurs because the CaO content of the liquid increases when olivine is the sole crystallizing silicate phase and because the D_{CaO} increases as the olivine Mg# decreases. Lower olivine

CaO contents than predicted by the crystallization trend should only be produced if the olivine equilibrates with either a liquid that has begun to fractionate plagioclase or if the olivine remains in equilibrium with a highly magnesian liquid that is lower in CaO than the melt from which it initially crystallized. A number of lines of evidence suggest that the low CaO contents of these olivines represent re-equilibration of the olivine with a highly magnesian liquid during residence inside the volcano. First, the crystallization of significant amounts of plagioclase would likely produce olivines with even lower olivine contents than seen in the horizontal trends in Figure 9. Examples of this behavior can potentially be seen in some samples from Loihi (Figure 9) and from post-shield dunites from Hualalai (Chen et al., 1992; Clague and Denlinger, 1994) which show lower CaO contents than most of the olivines discussed here. In both cases, these olivines likely equilibrated with liquids that had crystallized significant amounts of plagioclase and were therefore low in total CaO. These liquids are likely not common during the main shield-building stage because of the higher magma flux. Second, we have additional evidence for the MgO content of the liquid that cumulate olivines equilibrated with provided by the histograms of olivine compositions (Figure 5). A smooth fractional crystallization trend in a Hawaiian basalt produces more high Mg# olivine than low Mg# olivine, but the change in weight fraction is small (Figure 10) and the large single peak close to the average composition would not be produced by simple crystallization. The large peak in olivine modal abundances likely reflects re-equilibration between the olivines and their host liquid. In a cumulate pile, the fraction of olivine would be large relative to the fraction of liquid, and due to diffusive exchange of FeO and MgO the olivines in the pile

would approach the average composition across the full pile, creating the large peak in olivine Mg# close to the average olivine composition. Diffusion of FeO and MgO in olivine is expected to be fast relative to CaO diffusion (Jurewicz and Watson, 1988b; Coogan et al., 2005), thus if the CaO contents of the olivines are able to diffusively equilibrate with their host liquid, FeO and MgO should as well.

Mauna Kea and Loihi each show significant quantities of olivine with higher CaO content, and Mauna Loa shows a small quantity as well. These olivines could potentially represent olivines that have not fully re-equilibrated by diffusion. For Mauna Kea and Mauna Loa, the existence of these olivines may suggest that they were formed and erupted during periods of high magma flux, as discussed previously, such that they did not have a long enough residence time for their CaO contents to re-equilibrate. For Loihi, conversely, these olivines may suggest that there currently is not yet a single, integrated magma chamber through which every liquid passes, and as such there may be no large cumulate pile in which the majority of the olivines can re-equilibrate.

This model makes a number of predictions for the CaO contents of Hawaiian olivines, some of which can be tested. In particular, it predicts that the maximum CaO content in an olivine should be found in crystals that form from lavas just before they reach plagioclase saturation. Microphenocrysts and core to rim transects across single grains could be expected to show high CaO contents without time for equilibration, but only if they formed before the onset of plagioclase crystallization (which could obscure this trend). Some microphenocrysts from the Pu'u O'o eruption do in fact show elevated CaO contents up to 0.48% CaO in a microphenocryst with Mg#=81.2 (Garcia et al.,

2000). Based on the other available olivine analyses, this measured composition is unexpected other than through a crystallization path as suggested by Libourel (1999). Yang et al. (1994) also examined CaO contents in some olivines from Mauna Kea, and found them to be consistent with the model of Jurewicz and Watson (1988a), which predicts a similar evolution to the model of Libourel (1999). Currently, the literature contains very few analyses of CaO contents in olivine microphenocrysts or of transects across single olivine grains that include CaO contents, and thus a full test of this model is currently difficult, although it does appear consistent with the available data.

4. DISCUSSION

4.1. Olivine accumulation within Hawaiian volcanoes

In virtually every Hawaiian volcano considered here, the average erupted liquid has significantly lower wt. % MgO than the calculated parental liquid. This result requires that some portion of the original mass of liquid entering the volcano remains deposited within the volcano as crystallized olivine, consistent with the geophysical evidence for olivine cumulates (Kauahikaua et al., 2000). Based on more limited previously available data sets, estimates of the average weight fraction of the total mass entering the volcano that has been deposited within Mauna Kea and Kilauea as olivine cumulates have been calculated (Clague and Denlinger, 1994; Baker et al., 1996). Using the larger data sets available here, we have repeated this calculation based on our olivine addition trends. While this number can only be considered an estimate, as the exact ratio depends on the exact composition of liquid entering and of olivine deposited within the volcano, it still appears to provide insight into volcanic development.

The results of our calculations are given in Table 5, along with the previous estimates of Clague and Denlinger (1994) and Baker et al. (1996). For both Kilauea and Mauna Kea, our estimate of the deposited mass is consistent with the numbers calculated in the earlier estimates. This analysis confirms several of the details discussed previously; both the Mauna Loa and Mauna Kea samples from the HSDP2 drill core have lost less olivine than typical samples from Kilauea or the KSDP core. The historic samples from Mauna Loa contain less olivine on average than those at the drill site, having lost an additional 7.8% of their mass on average. The historic flows from Kilauea, the Pu'u O'o eruption of Kilauea, and the SOH-1 drill core set have lost similar amounts of their mass as olivine; on average roughly 20% of the mass currently entering Kilauea is deposited within the volcano as accumulated olivine. The samples from the KSDP drill core have also lost a similarly large amount of olivine.

The alternate calculations and stratigraphic variation from Mauna Kea produce some interesting results in this calculation. As noted previously, we performed several different olivine addition calculations on Mauna Kea to try to fit the accumulated olivine composition. Using a higher MgO parental liquid (with ~19% MgO) requires up to 9% of the initial liquid mass to be deposited within the volcano to produce the drill core. In addition, the stratigraphic details in the HSDP2 core revealed sections with low and high wt % MgO over long durations. The upper submarine section of Mauna Kea, covering 67 k.y., has on average lost virtually zero olivine (based on the liquids from Table 4b). The lower portion of the submarine section, covering 80 k.y., has on average lost up to 12.7% of its mass as accumulated olivine.

4.2. Chronological trends in olivine abundance

The chronological variations in olivine abundance expressed in the drill cores provide a previously unavailable view into the development of Hawaiian volcanoes. Mauna Kea, Mauna Loa, and Ko'olau all show fairly high-frequency variations in olivine abundance at their drill sites later in their life. Successive flows likely reach each site on the order of a thousand years apart, based on the calibrated timescales, and as the volcanic activity wanes, an olivine-poor flow will be followed by a highly olivine-rich flow with seemingly no consistent pattern. The older, submarine section of Mauna Kea shows a different pattern with less variation between successive flows. The upper portion of the core is highly olivine-rich, and there is a long-term trend towards less olivine deeper in the core.

Garcia et al. (2007) noted that the HSDP drill cores through Mauna Loa and Mauna Kea were much more olivine-rich than the SOH-1 drill core through Kilauea, which they related to the locations of the drill cores. The SOH-1 core was drilled far down the East Rift zone of Kilauea where eruptions are less frequent, and the low olivine abundances were interpreted to be caused by longer periods of magma storage prior to eruption at those distances from the summit, giving crystals more time to settle out. If that were the main mechanism driving the increasing olivine abundance with time in Mauna Kea, it would imply that the residence time for magmas in the lower section of the core is greater than that found in the upper submarine section of the core and that the eruptive rate peaks just before the submarine to subaerial transition. This timetable differs from the growth model for Mauna Kea of Sharp and Renne (2005), which used a linear

fit to describe accumulation at the drill site through the submarine section and a decreasing accumulation rate thereafter.

Rhodes and Vollinger (2004) noted the increasing whole rock MgO content in the upper portion of the submarine Mauna Kea section and proposed that the increasing MgO content reflected a period of high magma flux. During times of high magma flux, the parental liquids entering the volcano may not have sufficient time to crystallize to the point where they reach saturation with additional phases. However, a higher MgO content in the erupted liquids does not explain the change in whole-rock MgO content without the entrainment of additional olivine, for several reasons. As noted previously, one method of fitting the average olivine composition sampled by Mauna Kea is to interrupt olivine phenocryst crystallization with ~9% MgO in the liquid, rather than at ~7% MgO where other phases become saturated (e.g., Rhodes and Vollinger, 2004). This increased liquid MgO content would be consistent with the observation of Rhodes and Vollinger (2004) that there are very few whole rock analyses with <8% MgO throughout much of the submarine section. However, the upper portion of the submarine section shows a much larger increase in whole rock MgO content than the change from 7 to 9% MgO we calculate for the liquid compositions, and there are very few glasses measured from the HSDP2 section with >9% MgO (Stolper et al., 2004). Eruption of liquids containing MgO contents greater than this amount would produce elevated whole rock MgO values without growing significant amounts of olivine phenocrysts, and as such would disturb the relationship between whole rock MgO content and olivine abundance seen in Figure 1. This pattern could possibly be masked by the growth of rims on previously crystallized

phenocrysts during eruption, but this type of growth may be observable by chemical analyses of other oxides (such as CaO and NiO). Therefore, while the liquids may be higher in MgO, significant additional olivine is still required to explain the whole rock measurements. This additional olivine may however still be related to elevated magma fluxes; increased magma flux could decrease the time available for olivine grains to settle out into a cumulate and could therefore produce more olivine-rich eruptions. A high magma flux through Mauna Kea during the period sampled in the upper submarine section at the HSDP2 drill site appears to be one explanation for the variation in olivine abundance with time seen in this drill core.

4.3. Olivine addition and equilibration

Rhodes and Vollinger (2004) argued that the olivine-addition calculations presented here may not be representative of the actual mixing process occurring within a Hawaiian volcano. Specifically, they noted that olivine addition trends involving oxides other than MgO and FeO* often projected towards compositions that could not represent a realistic olivine composition. They explained this by suggesting that the linear trends examined here were in fact mixing lines between olivine rich, high MgO liquids and low MgO liquids that had begun to crystallize plagioclase and clinopyroxene. The olivine compositions considered here suggest a possible alternative explanation.

Calculating the olivine composition being added along an olivine-control line involves projecting over a large range in composition space, such that small but consistent changes in the measured compositions could be magnified by the mathematical projection. In Figure 11 we consider the oxides CaO and Al₂O₃, as was done by Rhodes

and Vollinger (2004). In a similar plot, they noted that when projected back to zero Al_2O_3 (and hence, the average olivine composition), the olivine control lines projected to $>0.4\%$ CaO, which is an implausible olivine composition for Hawaii, as discussed earlier. However, this extrapolation presupposes that there is no re-equilibration between the olivine and the liquid hosting it. In Figure 11, we also show an olivine control line that would be generated by an increase from 10.2% CaO to 10.4% CaO in the high MgO parental liquid if it was not accompanied by an increase in the CaO content of the fractionated liquid. This small increase in the CaO content of the high MgO liquids in the volcano produces a similar increase in the estimated CaO content of the olivine to that discussed by Rhodes and Vollinger (2004).

The olivine compositions examined in Figure 9 provide a possible mechanism for producing this exact type of enrichment. As noted previously, based on the work of Libourel (1999), a typical fractional crystallization trend in a Hawaiian liquid would be expected to produce olivines with $>0.4\%$ CaO when their Mg# approached 80, but olivines of this CaO content are typically not seen in Hawaii and there is a strong suggestion that the olivine CaO contents have undergone diffusive re-equilibration. CaO is relatively incompatible in olivine, and thus diffusive equilibration between olivine and liquid will increase the CaO content of the liquid slightly as the CaO content of the olivine decreases. This effect will be small, but it would be expected to be most prominent in a setting where the mass ratio of olivine to liquid is high, such as a cumulate pile of the sort envisioned here. The effect noted by Rhodes and Vollinger (2004) was

found to be more intense in Mauna Loa than Mauna Kea, which is also consistent with the greater intensity of olivine CaO depletion observed in olivines from Mauna Loa.

The proposed re-equilibration mechanism would work similarly for a number of other oxides. NiO, for example, is compatible in olivine, and crystallization of a liquid should produce a decrease in olivine NiO content as crystallization proceeds. Like MgO, the olivine addition calculation predicts a smooth decrease in the NiO content of olivines as crystallization proceeds. Like MgO however, a histogram of the measured NiO contents shows a large population of olivines around ~0.4% NiO, and few olivines at the tails of the distribution (Figure 12), suggesting that re-equilibration of NiO contents is plausible as well.

If this mechanism is an appropriate explanation for the variable projected olivine compositions from Rhodes and Vollinger (2004), it removes one of the concerns expressed over this type of calculation; that the variability seen in projected olivine composition could reflect mixing between high MgO liquids and liquids that had begun to crystallize other minerals. It does, however, suggest that care must be taken to understand the changes in each oxide in olivine during the olivine addition calculations. For example, assuming an increasing CaO content in olivine with increasing Mg# may be appropriate in some settings, but here, many of the olivines have re-equilibrated to a lower CaO content independent of Mg#, and therefore assuming that olivine CaO content was changing significantly during crystallization would produce a slightly erroneous parental liquid CaO content.

If this proposed mechanism is the correct way to explain the olivine compositions discussed above, it also potentially gives insight into the question of the exact relationship between olivines and their host liquid. As discussed previously, a number of lines of evidence suggest that some fraction of the olivines in any given Hawaiian lava have likely spent some time residing in a cumulate pile at the base of a magma chamber. Many studies have based their conclusions on compositional analyses of olivine grains or on bulk analyses of olivine separates (e.g., Sobolev et al., 2007; Eiler et al., 1996; Wang et al., 2003). A close relationship between olivines and their host melts is a common assumption of these studies, and is supported by the fact that there are correlations between measurements from whole rocks and measurements made on olivine separates (e.g., Blitchert-Toft et al., 2003; Kurz et al., 2004). As the olivine CaO content measurements appear to reflect varying degrees of diffusive re-equilibration, CaO content measurements in olivine provide a potential method for discriminating olivines that moved rapidly through the magma chamber from those that resided for long periods in a magma chamber. Jurewicz and Watson (1988b) measured MgO diffusion in olivine that was a factor of ~10 faster than CaO diffusion in olivine, and suggested that typical phenocrysts may take only a few years to fully re-equilibrate in Fe-Mg. Therefore, while Fe-Mg zonation in olivines would be difficult to preserve even in olivine phenocrysts that moved rapidly through the magmatic system, the preservation of high CaO contents in olivines such as those from Mauna Kea suggests that the high CaO fraction of olivines is able to move through the magma chamber more rapidly than other grains from the same flows. Based on the expected evolution of olivine CaO contents from Libourel (1999), it

appears possible to separate olivines that show substantial re-equilibration from those that do not. Therefore, the CaO content of olivines could be used as a potential discriminant to separate olivines that spent significant time residing in a cumulate pile from those that are more directly related to the lavas that host them; olivines that sit closest to the trend predicted by Libourel (1999) would likely have spent the least time residing in a magma chamber.

5. ACKNOWLEDGEMENTS

This work was supported by the NSF Ocean Sciences Marine Geology and Geophysics program, grant numbers OCE-0241716 and OCE-0550216.

References

- Althaus, T., Niedermann, S., and Erzinger, J. (2003) Noble gases in olivine phenocrysts from drill core samples of the Hawaii Scientific Drilling Project (HSDP) pilot and main holes (Mauna Loa and Mauna Kea, Hawaii). *Geochem. Geophys. Geosyst.* **4**, 8701.
- Anderson, A. T. (1995) CO₂ and the eruptibility of picrite and komatiite. *Lithos* **34**, 19-25.
- Arevalo, R. and McDonough, W. F. (2008) Tungsten geochemistry and implications for understanding the Earth's interior. *Earth Planet Sc. Lett.* **272**, 656-665.
- Baker, M. B., Alves, S., and Stolper, E. M. (1996) Petrography and petrology of the Hawaii Scientific Drilling Project lavas: inferences from olivine phenocryst abundances and compositions. *J. Geophys. Res.* **101**, 11715-11727.
- Basaltic Volcanism Study Project. (1980) *Basaltic volcanism on the terrestrial planets*. Pergamon Press, New York.
- Beattie, P. (1993) Olivine-melt and orthopyroxene-melt equilibria. *Contrib. Mineral. Petr.* **115**, 103-111.
- Beeson, M. H. (1976) Petrology, mineralogy, and geochemistry of the East Molokai volcanic series, Hawaii, U.S. *U.S. Geological Survey Professional Paper* **961**, 1-53.
- Bergmanis, E. C., Sinton, J. M., and Trusdell, F. A. (2000) Rejuvenated volcanism along the southwest rift zone, East Maui, Hawai'i. *B. Vulcanol.* **62**, 239-255.

- Blichert-Toft, J., Weis, D., Maerschalk, C., Agranier, A., and Albarède, F. (2003) Hawaiian hot spot dynamics as inferred from the Hf and Pb isotope evolution of Mauna Kea volcano. *Geochem. Geophys. Geosyst.* **4**, 8704.
- Bohrson, W. A. and Clague, D. A. (1988) Origin of ultramafic xenoliths containing exsolved pyroxenes from Hualalai Volcano, Hawaii *Contrib. Mineral. Petr.* **100**, 139-155.
- Budahn, J. R. and Schmitt, R. A., 1985. Petrogenetic modeling of Hawai'ian tholeiitic basalts: a geochemical approach. *Geochim Cosmochim Ac.* **49**, 67-87.
- Burkhard, D. J. M. (2001) Crystallization and oxidation of Kilauea Basalt glass: processes during reheating experiments. *J. Petrol.* **42**, 507-527.
- Casadevall, T. J. and Dzurisin, D. (1987) Stratigraphy and petrology of the Uwekahuna bluff section, Kilauea Caldera. *U.S. Geological Survey Professional Paper* **1350**, 351-375.
- Casadevall, T. J. and Dzurisin, D. (1987) Intrusive rocks of Kilauea Caldera. *U.S. Geological Survey Professional Paper* **1350**, 377-394.
- Chen, C. Y., Frey, F. A., and Garcia, M. O. (1990) Evolution of alkalic lavas at Haleakala volcano, East Maui, Hawai'i: major, trace element, and isotopic constraints. *Contrib. Mineral. Petr.* **105**, 197-218.
- Chen, C. Y., Frey, F. A., Garcia, M. O., Dalrymple, G. B., and Hart, S. R. (1991) The tholeiite to alkalic basalt transition at Haleakala volcano, Maui, Hawai'i. *Contrib. Mineral. Petr.* **106**, 183-200.

- Chen, C. H., Presnall, D. C., and Stern, R. J. (1992) Petrogenesis of ultramafic xenoliths from the 1800 Kaupulehu Flow, Hualalai Volcano, Hawaii. *J. Petrology* **33**, 163-202.
- Chen, C. Y. (1993) High-magnesium primary magmas from Haleakala Volcano, East Maui, Hawai'i: petrography, nickel, and major element constraints. *J. Volcanol. Geoth. Res.* **55**, 143-153.
- Chen, C. Y., Frey, F. A., Rhodes, J. M., and Easton, R. M. (1996) Temporal geochemical evolution of Kilauea Volcano: comparison of Hilina and Puna basalt. In: *Earth Processes: Reading the Isotopic Code*. (eds. Basu, A. and Hart, S. R.), American Geophysical Union, Washington D.C. pp. 161-181.
- Clague, D. A. and Beeson, M. H. (1980) Trace element geochemistry on the East Molokai Volcanic Series, Hawaii. *Am. J. Sci.* **280-A**, 820-844.
- Clague, D. A., Chen, D.-G., Murnane, R., Beeson, M. H., Lanphere, M. A., Dalrymple, G. B., Friesen, W. B., and Holcomb, R. T., 1982. Age and petrology of the Kalaupapa Basalt, Molokai, Hawaii. *Pac. Sci.* **36**, 411-420.
- Clague, D. A. and Frey, F. A. (1982) Petrology and trace element geochemistry of the Honolulu volcanic series, Oahu: implications of the oceanic mantle beneath Hawai'i. *J. Petrol.* **23**, 447-504.
- Clague, D. A. (1988) Petrology of ultramafic xenoliths from Loihi seamount, Hawai'i. *J. Petrol.* **29**, 1161-1186.
- Clague, D. A. and Moore, J. G. (1991) Geology and petrology of Mahukona Volcano, Hawai'i. *B. Volcanol.* **53**, 159-172.

- Clague, D. A. and Bohrsen, W. A. (1991) Origin of xenoliths in the trachyte at Puu Waawaa, Hualalai Volcano, Hawaii. *Contrib. Mineral. Petr.* **108**, 439-452.
- Clague, D. A., Weber, W. S., and Dixon, J. E. (1991) Picritic glasses from Hawaii. *Nature* **353**, 553-556.
- Clague, D. A. and Denlinger, R. P. (1994) Role of olivine cumulates in destabilizing the flanks of Hawaiian volcanoes. *B. Vulcanol.* **56**, 425-434.
- Clague, D. A., Moore, J. G., Dixon, J. E., and Friesen, W. B. (1995) Petrology of submarine lavas from Kilauea's Puna Ridge, Hawai'i. *J. Petrol.* **36**, 299-349.
- Clague, D. A. and Moore, J. G. (2002) The proximal part of the giant submarine Wailau Landslide, Molokai, Hawai'i. *J. Volcanol. Geoth. Res.* **113**, 259-287.
- Clague, D. A. P., J.B., McIntosh, W. C., Cousens, B. L., Davis, A. S., and Reynolds, J. R. (2006) A submarine perspective of the Honolulu volcanics, Oahu. *J. Volcanol. Geoth. Res.* **151**, 279-307.
- Coogan, L. A., Hain, A., Stahl, S., and Chakraborty, S. (2005) Experimental determination of the diffusion coefficient for calcium in olivine between 900°C and 1500°C. *Geochim Cosmochim Ac.* **69**, 3683-3694.
- Coombs, M. L., Clague, D. A., Moore, G. F., and Cousens, B. (2004) Growth and collapse of Waianae volcano, Hawai'i, as revealed by exploration of its submarine flanks *Geochemistry, Geophysics, Geosystems*, Q8006.
- Crocket, J. H. (2002) Platinum-group elements in basalts from Maui, Hawai'i: low abundances in alkali basalts. *Can. Mineral.* **40**, 595-609.

- Davis, M. G., Garcia, M. O., and Wallace, P. J. (2003) Volatiles in glasses from Mauna Loa Volcano, Hawai'i: implications for magma degassing and contamination, and growth of Hawai'ian volcanoes. *Contrib. Mineral. Petr.* **144**, 570-591.
- Decker, R. W. (1987) Dynamics of Hawaiian volcanoes: an overview. *U.S. Geological Survey Professional Paper 1350*, 997-1018.
- DePaolo, D. J., Stolper, E. M., and Thomas, D. (1996) The Hawaii Scientific Drilling Project: Summary of preliminary results. *GSA today* **6**, 1-8.
- DePaolo, D. J. and Stolper, E. M. (1996) Models of Hawaiian volcano growth and plume structure: Implications of results from the Hawaii Scientific Drilling Project. *J. Geophys. Res.* **101**, 11643-11654.
- Desilets, D. and Zreda, M. G. (2006) Elevation dependence of cosmogenic ^{36}Cl production in Hawai'ian lava flows. *Earth Planet Sc. Lett.* **246**, 277-287.
- Dixon, J. E. and Clague, D. A. (2001) Volatiles in basaltic glasses from Loihi seamount, Hawai'i: evidence for a relatively dry plume component. *J. Petrol.* **42**, 627-654.
- Dixon, J., Clague, D. A., Cousens, B., Monsalve, M. L., and Uhl, J. (2008) Carbonatite and silicate melt metasomatism of the mantle surrounding the Hawaiian plume: Evidence from volatiles, trace elements, and radiogenic isotopes in rejuvenated-stage lavas from Niihau, Hawaii. *Geochem. Geophys. Geosyst.* **9**, Q09005.
- Dzurisin, D., Lockwood, J. P., Casadevall, T. J., and Rubin, M. (1995) The Uwekahuna Ash Member of the Puna Basalt: product of violent phreatomagmatic eruptions at Kilauea Volcano Hawai'i between 2800 and 2100 years ago. *J. Volcanol. Geoth. Res.* **66**, 163-184.

- Eason, R. M. and Garcia, M. O. (1980) Petrology of the Hilina formation, Kilauea volcano, Hawai'i. *B. Vulcanol.* **43**, 657-673.
- Eiler, J. M., Valley, J. W., and Stolper, E. M. (1996) Oxygen isotope ratios in olivine from the Hawaii Scientific Drilling Project. *J. Geophys. Res.* **101**, 11807-11813.
- Feigenson, M. D. and Spera, F. J., 1983. Case studies on the origin of basalt II: the transition from tholeiitic to alkalic volcanism on Kohala volcano, Hawai'i. *Contrib. Mineral. Petr.* **84**, 390-405
- Fekiacova, Z., Abouchami, W., Galer, S. J. G., Garcia, M. O., and Hofmann, A. W. (2007) Origin and temporal evolution of Ko'olau volcano: Hawai'i: inferences from isotope data on the Ko'olau Scientific Drilling Project (KSDP), the Honolulu volcanics and ODP site 843. *Earth Planet Sc. Lett.* **261**, 65-83.
- Fiske, R. S. and Koyanagi, R. Y. (1968) The December, 1965 eruption of Kilauea Volcano, Hawai'i. *U.S. Geological Survey Professional Paper* **607**, 1-21.
- Fleet, M. E. and Stone, W. E. (1990) Nickeliferous sulfides in xenoliths, olivine megacrysts and basaltic glass. *Contrib. Mineral. Petr.* **105**, 629-636.
- Fodor, R. V. and Vandermeijden, H. J. (1988) Petrology of Gabbroic Xenoliths From Mauna Kea Volcano, Hawaii. *J. Geophys. Res.* **93**, 4425-4452.
- Fodor, R. and Moore, R. (1994) Petrology of gabbroic xenoliths in 1960 Kilauea basalt: crystalline remnants of prior (1955) magmatism. *B. Vulcanol.* **56**, 62-74.
- Fodor, R. V. and Galar, P. (1997) A view into the subsurface of Mauna Kea volcano, Hawai'i: crystallization processes interpreted through the petrology and petrography of gabbroic and ultramafic xenoliths. *J. Petrol.* **38**, 581-624.

- Frey, F. A. and Clague, D. A. (1983) Geochemistry of diverse basalt types from Loihi Seamount, Hawai'i, petrogenic implications. *Earth Planet Sc. Lett.* **66**, 337-355.
- Frey, F. A., Wise, W. S., Garcia, M. O., Kwon, S.-T., and Kennedy, A. K. (1990) Evolution of Mauna Kea volcano, Hawai'i: petrologic and geochemical constraints on postshield volcanism. *J. Geophys. Res.* **B95**, 1271-1300.
- Frey, F. A., Garcia, M. O., Wise, W. S., Kennedy, A. K., Gurriet, P., and Albarède, F. (1991) The evolution of Mauna Kea volcano, Hawai'i: Petrogenesis of tholeiitic and alkalic basalts. *J. Geophys. Res.* **B96**, 14347-14375.
- Frey, F. A., Garcia, M. O., and Roden, M. F. (1994) Geochemical characteristics of Ko'olau volcano: implications of intershield geochemical differences among Hawai'ian volcanoes. *Geochim Cosmochim Ac.* **58**, 1441-1462.
- Gaffney, A. M. (2002) Environments of crystallization and compositional diversity of Mauna Loa xenoliths. *J. Petrol.* **43**, 963-980.
- Gaffney, A. M., Nelson, B. K., and Blichert-Toft, J. (2004) Geochemical constraints on the role of oceanic lithosphere in intra-volcano heterogeneity at West Maui, Hawai'i. *J. Petrol.* **45**, 1663-1687.
- Garcia, M. O. and Wolfe, E. W. (1988) Petrology of the erupted lava. *U.S. Geological Survey Professional Paper* **1463**, 127-143.
- Garcia, M. O., Ho, R. A., Rhodes, J. M., and Wolfe, E. W. (1989) Petrologic constraints on rift-zone processes - results from episode-1 of the Pu'u O'o eruption of Kilauea volcano, Hawai'i. *B. Vulcanol.* **52**, 81-96.

- Garcia, M. O., Muenow, D. W., Aggrey, K. E., and O'Neil, J. R. (1989) Major element, volatile, and stable isotope geochemistry of Hawaiian submarine tholeiitic glasses. *J. Geophys. Res.* **94**, 10525-10538.
- Garcia, M. O., Rhodes, J. M., Wolfe, E. W., Ulrich, G. E., and Ho, R. A. (1992) Petrology of lavas from episodes 2-47 of the Pu'u O'o eruption of Kilauea volcano, Hawai'i: evaluation of magmatic processes. *B. Vulcanol.* **55**, 1-16.
- Garcia, M. O., Foss, D. J. P., West, H. B., and Mahoney, J. J. (1995) Geochemical and isotopic evolution of Loihi Volcano, Hawaii. *J. Petrol.* **36**, 1647-1674.
- Garcia, M. O., Hulsebosch, T. P., and Rhodes, J. M. (1995) Olivine-rich submarine basalts from the southwest rift zone of Mauna Loa volcano: implications for magmatic processes and geochemical evolution. In: *Mauna Loa Revealed: Structure, Composition, History, and Hazards* (eds. Rhodes, J. M. and Lockwood, J. P.) *Geophys. Monogr. Ser.*, vol.92. AGU, Washington D.C. pp. 219-239.
- Garcia, M. O. (1996) Petrography and olivine and glass chemistry of lavas from the Hawaii Scientific Drilling Project. *J. Geophys. Res.* **101**, 11701-11713.
- Garcia, M. O., Rhodes, J. M., Trusdell, F. A., and Pietruska, A. J. (1996) Petrology of lavas from the Pu'u'O'o eruption of Kilauea volcano - 3 - the Kupaianaha episode (1986-1992). *B. Vulcanol.* **58**, 359-379.
- Garcia, M. O., Ito, E., Eiler, J. M., and Pietruska, A. J. (1998) Crustal contamination of Kilauea Volcano magma revealed by oxygen isotope analyses of glass and olivine from Pu'u O'o eruption lavas,. *J. Petrol.* **39**, 803-817.

- Garcia, M. O., Rubin, K. H., Norman, M. D., Rhodes, J. M., Graham, D. W., Muenow, D. W., and Spencer, K. (1998) Petrology and geochronology of basalt breccia from the 1996 earthquake swarm of Loihi seamount, Hawaii: magmatic history of its 1996 eruption. *B. Volcanol.* **59**, 577-592.
- Garcia, M. O., Pietruska, A. J., Rhodes, J. M., and Swanson, K. (2000) Magmatic Processes during the prolonged Pu'u 'O'o eruption of Kilauea Volcano, Hawai'i. *J. Petrol.* **41**, 967-990.
- Garcia, M. O. and Pietruska, A. J. R., J.M. (2003) A petrologic perspective of Kilauea volcano's summit magma reservoir. *J. Petrol.* **44**, 2313-2339.
- Garcia, M. O., Haskins, E. H., Stolper, E. M., and Baker, M. (2007) Stratigraphy of the Hawai'i Scientific Drilling Project core (HSDP2): anatomy of a Hawaiian shield volcano. *Geochem. Geophys. Geosyst.* **8**, Q02G20.
- Garcia, M. O., Ito, E., and Eiler, J. M. (2008) Oxygen isotope evidence for chemical interaction of Kilauea historical magmas with basement rocks. *J. Petrol.* **49**, 757-769.
- Gerlach, T. M. and Graeber, E. J. (1985) Volatile budget of Kilauea volcano. *Nature* **313**, 273-277.
- Guillou, H., Garcia, M. O., and Turpin, L. (1997) Unspiked K-Ar dating of young volcanic rocks from Loihi and Pitcairn hot spot seamounts. *J. Volcanol. Geoth. Res.* **78**, 239-249.

- Guillou, H., Sinton, J. M., Laj, C., Kissel, C., and Szeremeta, N. (2000) New K-Ar ages of shield lavas from Waianae volcano, Oahu, Hawaiian archipelago. *J. Volcanol. Geoth. Res.* **96**, 229-242.
- Gunn, B. M. (1971) Trace element partitioning during olivine fractionation of Hawai'ian basalts. *Chemical Geology* **8**, 1-13.
- Hammer, J. E., Coombs, M. L., Shamberger, P. J., and Kimura, J.-I. (2006) Submarine sliwer in North Kona: a window into the early magmatic and growth history of Hualalai Volcano, Hawai'i. *J. Volcanol. Geoth. Res.* **151**, 157-188.
- Haskins, E. H. and Garcia, M. O. (2004) Scientific drilling reveals geochemical heterogeneity within the Ko'olau shield, Hawai'i. *Contrib. Mineral. Petr.* **147**, 162-188.
- Hauri, E. H. and Kurz, M. D. (1997) Melt migration and mantle chromatography, 2: a time-series Os isotope study of Mauna Loa Volcano, Hawai'i. *Earth Planet Sc. Lett.* **153**, 21-36.
- Hawkins, J. and Melchoir, J. (1983) Petrology of Basalts from Loihi Seamount, Hawai'i. *Earth Planet Sc. Lett.* **66**, 356-368.
- Hay, R. L. and Iijima, A. (1968) Nature and origin of palagonite tuffs of the Honolulu group on Oahu, Hawai'i. *Memoirs of the Geological Society of America* **116**, 331-376.
- Helz, R. T. (1987) Diverse olivine types in lava of the 1959 eruption of Kilauea volcano and their bearing in eruption dynamics. *U.S. Geological Survey Professional Paper* **1350**, 691-721.

- Helz, R. T. and Wright, T. L. (1992) Differentiation and magma mixing on Kilauea's east rift zone: A further look at the eruptions of 1955 and 1960. I: The late 1955 lavas. *B. Vulcanol.* **54**, 361-384.
- Ho, R. A. and Garcia, M. O. (1988) Origin of differentiated lavas at Kilauea Volcano, Hawaii: Implications from the 1955 eruption. *B. Vulcanol.* **50**, 35-46.
- Huang, S. and Frey, F. A. (2003) Trace element abundances of Mauna Kea basalt from phase 2 of the Hawaii Scientific Drilling Project: Petrogenetic implications of correlations with major element content and isotopic ratios. *Geochem. Geophys. Geosyst.* **4**, 8711.
- Huang, S., Frey, F. A., Blichert-Toft, J., Fodor, R. V., Bauer, G. R., and Xu, G. (2005) Enriched components in the Hawaiian plume: evidence from Kahoolawe Volcano, Hawaii. *Geochem. Geophys. Geosyst.* **6**, Q11006
- Huang, S. C., Humayun, M., and Frey, F. A. (2007) Iron/manganese ratio and manganese content in shield lavas from Ko'olau Volcano, Hawai'i. *Geochim Cosmochim Acta.* **71**, 4557-4569.
- Jackson, E. D. and Wright, T. L. (1970) Xenoliths in the Honolulu volcanic series, Hawai'i. *J. Petrol.* **11**, 405-430.
- Jackson, M. C., Frey, F. A., Garcia, M. O., and Wilmoth, R. A. (1999) Geology and geochemistry of basaltic lava flows and dikes from the Trans-Koolau tunnel, Oahu, Hawai'i. *B. Vulcanol.* **60**, 381-401.

- Jurewicz, A. J. G. and Watson, E. B. (1988a) Cations in olivine, Part 1: calcium partitioning and calcium-magnesium distribution between olivines and coexisting melts, with petrologic applications. *Contrib. Mineral. Petr.* **99**, 176-185.
- Jurewicz, A. J. G. and Watson, E. B. (1988b) Cations in olivine, Part 2: diffusion in olivine xenocrysts, with applications to petrology and mineral physics. *Contrib. Mineral. Petr.* **99**, 186-201.
- Kauahikaua, J., Hildenbrand, T., and Webring, M. (2000) Deep magmatic structures of Hawaiian volcanoes, imaged by three-dimensional gravity models. *Geology* **28**, 883-886.
- Kilinc, A., Carmichael, I. S. E., Rivers, M. L., and Sack, R. O. (1983) The ferric-ferrous ratio of natural silicate liquids equilibrated in air. *Contrib. Mineral. Petr.* **83**, 136-140.
- Kimura, J.-I., Sisson, T. W. N., Nakano, Coombs, M. L., and Lipman, P. W. (2006) Isotope geochemistry of early Kilauea magmas from the submarine Hilina bench: the nature of the Hilina mantle component. *J. Volcanol. Geoth. Res.* **151**, 51-72.
- Kostera, A. Z. (1997) Mineralogy and petrology of xenoliths in the Huehue flows of Hualalai volcano, Hawaii. *Proceedings of the 10th Keck Research Symposium. Geol., Wooster, OH*, 215-218.
- Kuno, H., Yamasaki, K., Iida, C., and Nagashima, K. (1957) Differentiation of Hawai'ian Magmas. *Japanese Journal of Geology and Geography* **28**, 179-218.

- Kurz, M. D., Curtice, J., Lott, D. E., III, and Solow, A. (2004) Rapid helium isotopic variability in Mauna Kea shield lavas from the Hawaiian Scientific Drilling Project. *Geochem. Geophys. Geosyst.* **5**, Q04G14.
- Kyser, T. K., O'Neil, J. R., and Carmichael, I. S. E. (1981) Oxygen isotope thermometry of basic lavas and mantle nodules. *Contrib. Mineral. Petr.* **77**, 11-23.
- Kyser, T. K., O'Neil, J. R., and Carmichael, I. S. E. (1982) Genetic relations among basic lavas and ultramafic nodules: Evidence from oxygen isotope compositions. *Contrib. Mineral. Petr.* **81**, 88-102.
- Lanphere, M. A. and Frey, F. A. (1987) Geochemical evolution of Kohala volcano, Hawai'i. *Contrib. Mineral. Petr.* **95**, 100-113.
- Leeman, W. P. and Scheidegger, K. F. (1977) Olivine/liquid distribution coefficients and a test for crystal-liquid equilibrium. *Earth Planet Sc. Lett.* **35**, 247-257.
- Libourel, G. (1999) Systematics of calcium partitioning between olivine and silicate melt: implications for melt structure and calcium content of magmatic olivines. *Contrib. Mineral. Petr.* **136**, 63-80.
- Lipman, P. W., Banks, N. G., and Rhodes, J. M. (1985) Degassing-induced crystallization of basaltic magma and effects on lava rheology. *Nature* **317**, 604-607.
- Lipman, P. W., Rhodes, J. M., and Dalrymple, G. B. (1990) The Ninole basalt: implications for the structural evolution of Mauna Loa volcano, Hawai'i. *B. Vulcanol.* **53**, 1-19.

- Lipman, P. W., Sisson, T. W., Ui, T., and Naka, J. (2000) In search of ancestral Kilauea volcano. *Geology* **28**, 1079-1082.
- Lipman, P. W., Sisson, T. W., Coombs, M. L., Calvert, A., and Kimura, J. (2006) Piggyback tectonics: Long-term growth of Kilauea on the south flank of Mauna Loa. *J. Volcanol. Geoth. Res.* **151**, 73-108.
- Lockwood, J. P., Dvorak, J. J., English, T. T., Koyangi, R. Y., Okamura, A. T., Summers, M. L., and Tanigawa, W. R. (1987) Mauna Loa 1974-1984: a decade of intrusive and extrusive activity. *U.S. Geological Survey Professional Paper* **1350**, 537-570.
- Macdonald, G. A. (1942) Potash-oligoclase in Hawaiian Lavas. *Am. Mineral.* **27**, 793-800.
- Macdonald, G. A. and Powers, H. A. (1946) Contribution to the petrography of Haleakala volcano, Hawai'i. *Bull. Geol. Soc. Am.* **57**, 115-123.
- Macdonald, G. A. (1949) Petrography of the island of Hawaii. *U.S. Geological Survey Professional Paper 214-D*, 51-96.
- Macdonald, G. A. and Eaton, J. P. (1955) Hawai'ian volcanoes during 1953. *U.S. Geological Survey Bulletin* **1021-D**, 127-166.
- Macdonald, G. A. and Katsura, T. (1961) Variations in the lava of the 1959 eruption of Kilauea Iki. *Pac. Sci.* **15**, 358-369.
- Macdonald, G. A. and Eaton, J. P. (1964) Hawai'ian volcanoes during 1955. *U.S. Geological Survey Bulletin* **1171**, 1-170.
- Macdonald, G. A. and Katusra, T. (1964) Chemical composition of Hawai'ian lavas. *J. Petrol.* **5**, 82-133.

- Macdonald, G. A. (1968) Composition and origin of Hawai'ian Lavas. *Memoirs of the Geological Society of America* **116**, 477-522.
- Macdonald, G. A. (1968) A further contribution to the petrology of Haleakala Volcano, Hawai'i. *Bull. Geol. Soc. Am.* **79**, 877-887.
- Mangan, M. T., Heliker, C. C., Mattox, T. N., Kauahikaua, J. P., and Helz, R. T. (1995) Episode 49 of the Pu'u'O'o-Kupaianahana eruption of Kilauea Volcano - breakdown of a steady-state eruptive era. *B. Vulcanol.* **55**, 127-135.
- Marske, J. P., Pietruska, A. J., Weis, D., Garcia, M. O., and Rhodes, J. M. (2007) Rapid passage of a small-scale mantle heterogeneity through the melting regions of Kilauea and Mauna Loa volcanoes. *Earth Planet Sc. Lett.* **259**, 34-50.
- Marske, J. P., Garcia, M. O., Pietruska, A. J., Rhodes, J. M., and Norman, M. D. (2008) Geochemical variations during Kilauea's Pu'u 'O'o-eruption reveal a fine-scale mixture of mantle heterogeneities within the Hawai'ian plume. *J. Petrol.* **49**, 1297-1318.
- Martin, C. E. (1991) Osmium isotopic characteristics of mantle-derived rocks. *Geochim Cosmochim Ac.* **55**, 1421-1434.
- Matvenkov, V. V. and Sorokhtin, O. G. (1998) Petrological characteristics of the initial stages of interplate volcanism, Loihi (Hawai'i, Pacific Ocean). *Okeanologiya* **38**, 742-749.
- McCann, V. E. and Barton, M. (2005) Olivine-melt equilibrium and the oxygen fugacities of lavas from Hawai'i, EOS Transactions AGU. #V31B-0615 (abstr.).
- Moore, J. G. (1965) Petrology of deep sea basalt near Hawai'i. *Am. J. Sci.* **263**, 40-52.

- Moore, J. G. and Evans, B. W. (1967) The role of olivine in the crystallization of the prehistoric Makaopuhi tholeiitic lava lake, Hawaii. *Contrib. Mineral. Petr.* **15**, 202-223.
- Moore, J. G. and Koyanagi, R. Y. (1969) The October 1963 eruption of Kilauea Volcano, Hawai'i. *U.S. Geological Survey Professional Paper* **614-C**, 1-13.
- Moore, R. B., Helz, R. T., Dzurisin, D., Eaton, G. P., Koyanagi, R. Y., Lipman, P. W., Lockwood, J. P., and Puniwai, G. S. (1980) The 1977 eruption of Kilauea Volcano, Hawai'i. *J. Volcanol. Geoth. Res.* **7**, 189-210.
- Moore, R. B. (1983) Distribution of the differentiated tholeiite basalts on the lower East Rift Zone of Kilauea Volcano, Hawai'i: a possible guide to geothermal exploration. *Geology* **11**, 136-140.
- Moore, J. G. and Clague, D. A. (1987) Coastal lava flows from Mauna Loa and Hualalai volcanoes, Kona, Hawaii. *B. Vulcanol.* **49**, 752-764.
- Moore, J. G., Clague, D. A., Ludwig, K. R., and Mark, R. K. (1990) Subsidence and volcanism of the Haleakala Ridge, Hawaii. *J. Volcanol. Geoth. Res.* **42**, 273-284.
- Moore, J. G. and Clague, D. A. (1992) Volcano growth and evolution of the island of Hawaii. *Geol. Soc. Am. Bull.* **104**, 1471-1484.
- Moore, J. G., Bryan, W. B., Beeson, M. H., and Normark, W. R. (1995) Giant blocks in the South Kona landslide, Hawaii. *Geology* **23**, 125-128.
- Morgan, J. K., Moore, G. F., and Clague, D. A. (2003) Slope failure and volcanic spreading along the submarine south flank of Kilauea volcano, Hawai'i. *J. Geophys. Res.* **108**, 2415.

- Morgan, J. K., Clague, D. A., Borchers, D. C., Davis, A. S., and Milliken, K. L. (2007) Mauna Loa's submarine western flank: landsliding, deep volcanic spreading, and hydrothermal alteration. *Geochem. Geophys. Geosyst.* **8**, Q05002.
- Muir, I. D., Tilley, C. E., and Scoon, J. H. (1957) Contributions to the petrology of Hawaiian Basalts 1. The picrite-basalts of Kilauea. *Am. J. Sci.* **255**, 241-253.
- Muir, I. D. and Tilley, C. E. (1961) Mugearites and their place in alkali igneous rock series. *Journal of Geology* **69**, 186-203.
- Muir, I. D., Tilley, C. E., and Scoon, J. H. (1963) Contributions to the petrology of Hawai'ian basalts II: the tholeiitic basalts of Mauna Loa and Kilauea. *Am. J. Sci.* **261**, 111-128.
- Mukhopadhyay, S., Lassiter, J. C., Farley, K. A., and Bogue, S. W. (2003) Geochemistry of Kauai shield-stage lavas: Implications for the chemical evolution of the Hawaiian plume. *Geochem. Geophys. Geosyst.* **4**, 1009.
- Murata, K. J. and Richter, D. H. (1961) Magmatic differentiation in the Uwekahuna Laccolith, Kilauea Caldera, Hawai'i. *J. Petrol.* **2**, 424-437.
- Murata, K. J., Bastron, H., and Brannock, W. W. (1965) X-Ray determinative curve for Hawaiian olivines of composition Fo76-88. *U.S. Geological Survey Professional Paper 525-C*, C35-C37.
- Murata, K. J. and Richter, D. H. (1966) Chemistry of the lavas of the 1959-60 eruption of Kilauea Volcano, Hawai'i. *U.S. Geological Survey Professional Paper 537-A*, 1-26.

- Neal, C. A., Duggan, T. J., Wolfe, E. W., and Brandt, E. L. (1988) Lava samples, temperatures, and compositions. *U.S. Geological Survey Professional Paper* **1463**, 99-126.
- Nicholls, J. and Stout, M. Z. (1988) Picritic Melts in Kilauea--Evidence from the 1967-1968 Halemaumau and Hiiaka Eruptions. *J. Petrology* **29**, 1031-1057.
- Norman, M. D. and Garcia, M. O. (1999) Primitive magmas and source characteristics of the Hawai'ian plume: petrology and geochemistry of shield picrites. *Earth Planet Sc. Lett.* **168**, 27-44.
- Oze, C. and Winter, J. D. (2005) The occurrence, vesiculation, and solidification of dense blue glassy pahoehoe. *J. Volcanol. Geoth. Res.* **142**, 285-301.
- Powers, H. A. (1931) Chemical analyses of Kilauea Lavas. *Volcano Letters* **362**, 1-2.
- Quane, S. L., Garcia, M. O., Guillou, H., and Hulsebosch, T. P. (2000) Magmatic history of the east rift zone of Kilauea Volcano, Hawai'i, based on drill core SOH-1. *J. Volcanol. Geoth. Res.* **102**, 319-388.
- Ren, Z.-Y., Takahashi, E., Orihashi, Y., and Johnson, K. T. M. (2004) Petrogenesis of tholeiitic lavas from the submarine Hana Ridge. *J. Petrol.* **45**, 2067 - 2099.
- Rhoden, M. F., Frey, F. A., and Clague, D. A. (1984) Geochemistry of tholeiitic and alkalic lavas from the Ko'olau range, Oahu, Hawai'i: implications for Hawai'ian volcanism. *Earth Planet Sc. Lett.* **69**, 141-158.
- Rhodes, J. M. (1983) Homogeneity of lava flows: chemical data for historic Mauna Loa eruptions. *Proceedings fo the 13th Lunar and Planetary Sciences Conference, Part 2, J. Geophys. Res.* **Supplemental A 88**, 869-879.

- Rhodes, J. M. (1988) Geochemistry of the 1984 Mauna Loa eruption: implications for magma storage and supply. *J. Geophys. Res.* **93**, 4453-4466.
- Rhodes, J. M. (1995) The 1852 and 1868 Mauna Loa picrite eruptions: clues to parental magma compositions and the magmatic plumbing system In: Rhodes, J. M. and Lockwood, J. P. (Eds.), *Mauna Loa Revealed*. American Geophysical Union, Washington D.C. pp. 241-262.
- Rhodes, J. M. and Hart, S. R. (1995) Episodic trace element and isotopic variations in historical Mauna Loa lavas: implications for magma and plume dynamics. In: Rhodes, J. M. and Lockwood, J. P. (Eds.), *Mauna Loa Revealed*. American Geophysical Union, Washington D.C. pp. 263-288.
- Rhodes, J. M. (1996) Geochemical stratigraphy of lava flows sampled by the Hawai'i Scientific Drilling Project. *J. Geophys. Res.* **101**, 11729-11746.
- Rhodes, J. M. and Vollinger, M. J. (2004) Composition of basaltic lavas sampled by phase-2 of the Hawai'i Scientific Drilling Project: geochemical stratigraphy and magma types. *Geochemistry, Geophysics, Geosystems* **5**, Q03G13.
- Rhodes, J. M. and Vollinger, M. J. (2005) Ferric/ferrous ratios in 1984 Mauna Loa lavas: a contribution to understanding the oxidation state of Hawai'ian magmas. *Contrib. Mineral. Petr.* **149**, 666-674.
- Richter, D. H., Ault, W. U., Eaton, J. P., and Moore, J. G. (1965) The 1961 eruption of Kilauea Volcano, Hawai'i. *U.S. Geological Survey Professional Paper* **474-D**, 1-

- Richter, D. H. and Moore, J. G. (1966) Petrology of the Kilauea Iki lava lake, Hawai'i. *U.S. Geological Survey Professional Paper 537-B*, 1-26.
- Roeder, P. L., Thornber, C., Poustovetov, A., and Grant, A. (2003) Morphology and composition of spinel in Pu'u 'O'o lava (1996-1998), Kilauea volcano, Hawaii. *J. Volcanol. Geoth. Res.* **123**, 245-265.
- Roeder, P., Gofton, E., and Thornber, C. (2006) Cotectic proportions of olivine and spinel in olivine-tholeiitic basalt and evaluation of pre-eruptive processes. *J. Petrol.* **47**, 883-900.
- Ryan, M. P. (1988) The mechanics and three-dimensional internal structure of active magmatic systems; Kilauea volcano, Hawaii. *J. Geophys. Res.* **93**, 4213-4248.
- Sarbas, B. and Nohl, U. (2008) The GEOROC database as part of a growing geoinformatics network. In: Brady, S. R., Sinha, A. K., and Gunderson, L. C. Eds.), *Geoinformatics 2008 - Data to Knowledge, Proceedings: U.S. Geological Survey Scientific Investigations Report 2008 - 5172*.
- Seaman, C., Sherman, S. B., Garcia, M. O., Baker, M. B., Balta, B., and Stolper, E. (2004) Volatiles in glasses from the HSDP2 drill core. *Geochem. Geophys. Geosyst.* **5**, Q09G16.
- Scowen, P. A. H., Roeder, P. L., and Helz, R. T. (1991) Reequilibration of chromite within Kilauea Iki lava lake, Hawaii. *Contrib. Mineral. Petr.* **107**, 8-20.
- Self, S., Keszthelyi, L., and Thordarson, T. (1998) The importance of pahoehoe. *Annu. Rev. Earth Planet. Sci.* **26**, 81-110.

- Shamberger, P. J. and Hammer, J. E. (2006) Leucocratic and Gabbroic Xenoliths from Hualalai Volcano, Hawai'i. *J. Petrology* **47**, 1785-1808.
- Sharp, W. D. and Renne, P. R. (2005) The Ar-40/Ar-39 dating of core recovered by the Hawaii Scientific Drilling Project (phase 2), Hilo, Hawaii. *Geochem. Geophys. Geosyst.* **6**, Q04G17.
- Shepherd, E. S. (1938) The gases in rocks and some related problems. *Am. J. Sci.* **35A**, 311-351.
- Sherrod, D. A., Nishimitsu, Y., and Takahiro, T. (2003) New K-Ar ages and the geologic evidence against rejuvenated-stage volcanism at Haleakala, East Maui, a postshield-stage volcano of the Hawaiian chain. *Bull. Geol. Soc. Am.* **115**, 683-694.
- Sherrod, D. R., Murai, T., and Tagami, T. (2007) New K-Ar ages for calculating end-of-shield extrusion rates at West Maui volcano, Hawaiian island chain. *B. Vulcanol.*, 627-642.
- Sims, K. W. W., DePaolo, D. J., Murrell, M. T., Baldrige, W. S., Goldstein, S. J., Clague, D. A., and Jull, M. (1999) Porosity of the melting zone and variations in the solid mantle upwelling rate beneath Hawai'i: inferences from ^{238}U - ^{230}Th - ^{226}Ra and ^{235}U - ^{231}Pa disequilibria. *Geochim Cosmochim. Acta.* **63**, 4119-4138.
- Sobolev, A. V. and Nikogosian, I. K. (1994) Petrology of long-lived mantle plume magmatism: Hawai'i, Pacific, and Reunion Island, Indian Ocean. *Petrology* **2**, 111-144.

- Sobolev, A. V., Hofmann, A. W., Kuzmin, D. V., Yaxley, G. M., Arndt, N. T., Chung, S. L., Danyushevsky, L. V., Elliott, T., Frey, F. A., Garcia, M. O., Gurenko, A. A., Kamenetsky, V. S., Kerr, A. C., Krivolutsкая, N. A., Matvienkov, V. V., Nikogosian, I. K., Rocholl, A., Sigurdsson, I. A., Sushchevskaya, N. M., and Teklay, M. (2007) The amount of recycled crust in sources of mantle-derived melts. *Science* **316**, 412-417.
- Spengler, S. and Garcia, M. O. (1988) Geochemistry of the Hawi Lavas, Kohala Volcano, Hawai'i. *Contrib. Mineral. Petr.* **99**, 90-104.
- Stoll, B., Jochum, K. P., Herwig, K., Amini, M., Flanz, M., Kreuzburg, B., Kuzmin, D., Willbold, M., and Enzweiler, J. (2008) An automated iridium-strip heater for LA-ICP-MS bulk analysis of geological samples. *Geostand. Geoanal. Res.* **32**, 5-26.
- Stolper, E., Sherman, S., Garcia, M., Baker, M., and Seaman, C. (2004) Glass in the submarine section of the HSDP2 drill core, Hilo, Hawaii. *Geochem. Geophys. Geosyst.* **5**, Q07G15.
- Takahiro, T., Nishimitsu, Y., and Sherrod, D. A. (2003) Rejuvenated-stage volcanism after 0.6 M.Y. quiescence at West Maui volcano, Hawai'i: new evidence from K-Ar ages and chemistry of Lahaina volcanics. *J. Volcanol. Geoth. Res.* **120**, 207-214.
- Tanaka, R. N., E. and Takahashi, E. (2002) Geochemical evolution of Ko'olau volcano, Hawai'i, *Hawai'ian volcanoes, Deep Underwater Perspectives (Geophysical Monograph)*. American Geophysical Union.

- Tanaka, R. and Eizo, N. (2005) Boron isotopic constraints on the source of Hawai'ian shield lavas. *Geochim Cosmochim Ac.* **69**, 3385-3399.
- Teanby, N., Laj, C., Gubbins, D., and Pringle, M. (2002) A detailed palaeointensity and inclination record from drill core SOH1 on Hawaii. *Physics of The Earth and Planetary Interiors* **131**, 101-140.
- Thornber, C. R., Sherrod, D. R., Siems, D. F., Heliker, C. C., Meeker, G. P., Oscarson, R. L., and Kauahikaua, J. P. (2002) Whole-rock and glass major-element geochemistry of Kilauea Volcano, Hawaii, near-vent eruptive products: September 1994 through September, 2001. *U.S. Geological Survey Open File Report 02-17*, 1-9.
- Thornber, C. R., Heliker, C., Sherrod, D. R., Kauahikaua, J. P., Miklius, A., Okubo, P. G., Trusdell, F. A., Budahn, J. R., Ridley, W. I., and Meeker, G. P. (2003) Kilauea east rift zone magmatism: an episode 54 perspective. *J. Petrol.* **44**, 1525-1559.
- Thornber, C. R., Hon, K., Heliker, C. C., and Sherrod, D. A. (2003) A compilation of whole-rock and glass major-element geochemistry of Kilauea Volcano, Hawai'i, near-vent eruptive products: January 1983 through September 2001 *U.S. Geological Survey Open File Report 03-477*.
- Tilley, C. E. (1960) Kilauea Magma. *Geological Magazine* **97**, 494-497.
- Tilley, C. E. and Scoon, J. H. (1960) Differentiation of Hawai'ian basalts - some variants in lava suites of dated Kilauean eruptions. *J. Petrol.* **1**, 47-55.
- Tilley, C. E. and Scoon, J. H. (1961) Differentiation of Hawai'ian basalts; trends of Mauna Loa and Kilauea historic magma. *Am. J. Sci.* **259**, 60-68.

- Toplis, M. J. (2005) The thermodynamics of iron and magnesium partitioning between olivine and liquid: criteria for assessing and predicting equilibrium in natural and experimental systems. *Contrib. Mineral. Petr.* **149**, 22-39.
- Wang, Z. G., Kitchen, N. E., and Eiler, J. M. (2003) Oxygen isotope geochemistry of the second HSDP core. *Geochem. Geophys. Geosyst.* **4**, 29.
- Wang, Z. and Gaetani, G. A. (2008) Partitioning of Ni between olivine and siliceous eclogite partial melt: experimental constraints on the mantle source of Hawaiian basalts. *Contrib. Mineral. Petr.* **156**, 661-678.
- Wanless, V. D., Garcia, M. O., Rhodes, J. M., Weis, D., and Norman, M. D. (2006) Shield-stage alkalic volcanism on Mauna Loa volcano, Hawai'i. *J. Volcanol. Geoth. Res.* **151**.
- Wanless, V. D., Garcia, M. O., Trusdell, F. A., Rhodes, J. M., Norman, M. D., Weis, D. F., D.J., Kurz, M. D., and Guillou, H. (2006) Submarine radial vents on Mauna Loa volcano, Hawai'i. *Geochemistry, Geophysics, Geosystems* **7**, Q05001.
- Washington, H. S. (1923) Petrology of the Hawai'ian Islands I: Kohala and Mauna Kea. *Am. J. Sci.* **5**, 465-502.
- Washington, H. S. (1923) Petrology of the Hawai'ian Islands III: Kilauea and general petrology of Hawai'i. *Am. J. Sci.* **6**, 338-367.
- Weinstein, J. P., Fodor, R. V., and Bauer, G. R. (2004) Ko'olau shield basalt as xenoliths entrained during rejuvenated-stage eruptions: perspectives on magma mixing. *B. Volcanol.* **66**, 182-199.

- Wentworth, C. K. and Winchell, H. (1947) Ko'olau basalt series, Oahu, Hawai'i. *Bull. Geol. Soc. Am.* **58**, 49-77.
- West, H. B., Garcia, M. O., Frey, F. A., and Kennedy, A. K. (1988) Nature and cause of compositional variation among the alkalic cap lavas of Mauna Kea volcano, Hawai'i. *Contrib. Mineral. Petr.* **100**, 383-397.
- West, H. B., Garcia, M. O., Gerlach, D. C., and Romano, J. (1992) Geochemistry of tholeiites from Lanai, Hawai'i. *Contrib. Mineral. Petr.* **112**, 520-542.
- White, R. W. (1966) Ultramafic inclusions in basaltic rocks from Hawaii. *Contrib. Mineral. Petr.* **12**, 245-314.
- Wilkinson, J. F. G. and Hensel, H. D. (1988) The petrology of some picrites from Mauna Loa and Kilauea volcanoes, Hawai'i. *Contrib. Mineral. Petr.* **98**, 326-345.
- Winchell, H. (1947) Honolulu Series, Oahu, Hawai'i. *Bull. Geol. Soc. Am.* **58**, 1-48.
- Wolfe, E. W., Wise, W. S., and Dalrymple, G. B. (1997) The geology and petrology of Mauna Kea volcano, Hawai'i - a study of postshield volcanism. *U.S. Geological Survey Professional Paper* **1557**, 1-129.
- Wright, T. L., Kinoshita, W. T., and Peck, D. L. (1968) March 1965 eruption of Kilauea Volcano and the formation of Makaopuhi Lava Lake. *J. Geophys. Res.* **73**, 3181.
- Wright, T. L. (1971) Chemistry of Kilauea and Mauna Loa lava in space and time. *U.S. Geological Survey Professional Paper* **735**, 1-40.
- Wright, T. L. and Fiske, R. S. (1971) Origin of the differentiated and hybrid lavas of Kilauea Volcano, Hawai'i. *J. Petrol.* **12**, 1-65.

- Wright, T. L. and Okamura, R. T. (1977) Cooling and crystallization of tholeiitic basalt, 1965 Makaopuhi Lava Lake, Hawai'i. *U.S. Geological Survey Professional Paper* **1004**, 78p.
- Wright, T. L. and Peck, D. L. (1978) Crystallization and differentiation of the Alae Magma, Alae Lava Lake, Hawai'i. *U.S. Geological Survey Bulletin* **935-C**, 1-20.
- Wright, T. L. (1984) Origin of Hawai'ian tholeiite: a metasomatic model. *J. Geophys. Res.* **89**, 3233-3252.
- Wright, T. L. and Helz, R. (1996) Differentiation and magma mixing on Kilauea's east rift zone: A further look at the eruptions of 1955 and 1960. 2. The 1960 lavas. *B. Vulcanol.* **57**, 602-630.
- Xu, G. P., Frey, F. A., Clague, D. A., Weis, D., and Beeson, M. H. (2005) East Molokai and other Kea-trend volcanoes: Magmatic processes and sources as they migrate away from the Hawaiian hot spot. *Geochem. Geophys. Geosyst.* **6**, 28.
- Yang, H. J., Frey, F. A., Garcia, M. O., and Clague, D. A. (1994) Submarine lavas from Mauna Kea Volcano, Hawai'i: implications for Hawai'ian shield stage processes. *J. Geophys. Res.* **99**, 15577-15594.
- Yoder, H. S. J. and Tilley, C. E. (1962) Origin of basalt magmas: an experimental study of natural and synthetic rock systems. *J. Petrol.* **3**, 342-532.
- Yokose, H. and Lipman, P. W. (2004) Emplacement mechanisms of the South Kona slide complex, Hawai'i Island: sampling and observations by remotely operated vehicle Kaiko. *B. Vulcanol.* **66**, 569-584.

Yokose, H., Lipman, P. W., and Kanamatsu, T. (2005) Physical and chemical properties of submarine basaltic rocks from the submarine flanks of the Hawai'ian islands.

Mar. Geol. **219**, 173-193.

Zreda, M. G., Phillips, F. M., Elmore, D., Kubik, P. W., Sharma, P., and Dorn, R. I.

(1991) Cosmogenic chlorine-36 production rates in terrestrial rocks. *Earth Planet*

Sc. Lett. **105**, 94-109.

TABLES

Table 1: Available whole rock analyses

	Total points	Points after filtering
East Molokai	171	9
Haleakala	286	82
Hualalai	268	122
Kahoolawe	24	4
Kauai	27	10
Kilauea	3171	1959
Kohala	137	4
Ko'olau	436	128
Lanai	22	6
Loihi	84	15
Mahukona	19	16
Mauna Kea	1059	325
Mauna Loa	676	303
Niihau	44	11
Waianae	128	49
West Maui	94	35
West Molokai	104	0
Total	6750	3078

Table 1: Total available whole rock analyses for Hawaiian volcanoes and remaining data after filtering for alteration, alkalinity, and fractionation of mineral phases other than olivine. References in Supplementary Table 1, filtering process as described in text.

Table 2: Point count results from the HSDP2 Caltech Reference Suite

Sample #	Unit	Wt. % MgO	Matrix (Vol %)	Oliv. (Vol %)	Plag. (Vol %)	Pyr. (Vol %)	Ves. (Vol %)
SR238-0.0	96	18.38	63.4	30.1	0.9	0.0	5.5
	96	18.38	63.1	30.3	1.4	0.0	5.2
	96	18.38	66.5	26.5	1.1	0.0	5.9
	96	18.38	66.1	27.6	0.9	0.0	5.5
SR125-6.48	45	10.26	68.1	2.1	0.0	0.0	29.8
SR127-5.7	46	6.64	87.8	7.1	2.9	1.5	0.7
SR170-0.7	71	17.71	70.9	23.6	0.0	0.0	5.5
SR175-1.4	73	23.96	51.1	37.9	0.0	0.0	11.0
SR186-5.3	77	16.76	54.5	20.2	0.6	0.0	24.7
SR258-3.6	104	7.12	96.4	0.7	0.1	0.0	1.3
SR262-.6	105	15.32	61.2	14.4	0.0	0.0	24.4
SR267-6.85	107	23.16	61.7	33.4	0.0	0.0	4.9
SR279-4.7	113	11.94	80.9	2.8	0.1	0.0	16.1
SR306-9.7	120	13.47	68.8	10.2	0.0	0.1	20.8
SR310-5.7	123	14.98	77.4	11.7	0.3	0.0	10.6
SR331-9.7	128	20.65	67.3	30.6	0.0	0.0	2.1
SR344-3.1	134	8.53	86.3	3.0	0.0	0.0	10.7
SR363-7.4	141	18.2	62.2	21.3	0.0	0.0	16.5
SR392-5.35	148	21.62	70.2	22.1	0.0	0.0	7.7
SR399-2.4	150	28.68	40.2	39.5	0.0	0.0	20.3
SR407-3.2	154	18.74	68.0	24.9	0.0	0.0	7.1
SR425-6.0	158	7.49	68.4	7.0	2.4	0.0	22.2
SR433-5.7	161	9.59	78.8	7.1	0.1	0.0	13.9
SR447-7.0	168	7.99	80.1	1.3	0.0	0.0	18.6
SR455-7.4	179	26.01	45.2	42.7	3.2	0.3	8.6
SR462-2.0	181	8.54	93.0	3.5	0.7	0.0	2.7
SR502-5.1	191	26.46	55.0	40.4	0.9	0.0	3.6
SR548-9.9	199	19.52	73.4	26.6	0.0	0.0	0.0
SR560-7.6	202	19.09	70.1	29.6	0.0	0.0	0.3
SR582-10.4	207	19.62	71.4	28.4	0.0	0.0	0.1
SR604-2.9	217	11.63	95.8	4.2	0.0	0.0	0.0
SR630-6.4	224	18.32	76.5	23.3	0.0	0.0	0.3
SR649-5.9	234	13.76	87.5	12.5	0.0	0.0	0.0
SR650-7.9	236	13.83	83.4	15.9	0.1	0.0	0.6
SR691-8.8	251	11.31	88.4	11.6	0.0	0.0	0.0
SR743-14.00	280	16.66	79.7	20.1	0.0	0.0	0.2
SR756-14.1	284	18.91	77.8	21.0	1.2	0.0	0.0
SR846-18.8	304	12.19	95.6	2.0	0.0	0.0	2.4
SR855-.1	305	8.92	89.2	6.6	4.2	0.0	0.0
SR891-17.4	316	22.04	72.9	27.0	0.0	0.0	0.1

SR915-4.8	328	13.31	80.1	15.3	0.3	0.0	4.1
SR930-16.6	333	22.11	67.2	28.1	0.2	0.0	4.5
SR949-11.5	336h	9.32	99.6	0.4	0.0	0.0	0.0

Table 2: Mineral proportions and vesicle abundances based on 500-800 points per thin section. All phases <0.5 mm were counted as part of the groundmass. Whole-rock MgO content for each flow from Rhodes and Vollinger (2004). Abbreviations are Oliv, Olivine; Plag, plagioclase; Aug, augite; Ves, vesicles. Groundmass (vol %) = 100 – reported mineral and vesicle abundances.

Table 3: Olivine compositions from this study and the literature

	Average olivine	Highest Mg #	Reference for highest Mg# olivine
Mauna Loa	87.5(3)	91.2	Garcia and Hulsebosch, 1995
Hualalai	87.4(5)	91.2	Kuno, 1969
Kilauea	86.6(5)	90.7	Clague et al., 1991
Mauna Kea	87.9(6)	90.5	Frey et al., 1991, Sobolev et al., 2007
Ko'olau	86.2(3)	90.5	Sobolev and Nikogosian, 1994
Waianae	85.0(7)		
Haleakala	86.6(4)		
Loihi	87.2(12)		

Table 3: The average olivine composition was calculated via linear regression on the compiled data shown in Figure 2, projected back to its intercept with a curve representing the composition of the olivine end-member with some trace-constituents as described in the text and shown in Figure 3. The upper and lower limits were calculated by extending the curves calculated as the 95% confidence limits on the regression analysis to their intersection point with the olivine composition curve. The highest Mg # olivines are specified here for volcanoes that are involved in the olivine addition calculations, where analyses of glass are available and data coverage is best. Other volcanoes were examined, but were not included because of a lack of data points to define the olivine control line.

Table 4

4a	SiO ₂	TiO ₂	Al ₂ O ₃	Cr ₂ O ₃	FeO	MnO	NiO	MgO	CaO	Na ₂ O	K ₂ O	P ₂ O ₅		
Mauna Kea Low SiO ₂	48.96	2.64	13.93	0.10	11.48	0.17	0.008	7.73	11.43	2.40	0.42	0.22		
Mauna Kea High SiO ₂	51.20	2.48	13.55	0.10	11.32	0.17	0.008	7.42	10.61	2.22	0.38	0.20		
Mauna Loa	51.96	2.10	13.83	0.10	10.21	0.17	0.008	7.58	10.89	2.21	0.32	0.19		
Ko'olau	51.70	2.36	14.22	0.10	10.88	0.17	0.008	7.13	10.44	2.18	0.39	0.21		
Kilauea	51.01	2.47	13.52	0.10	10.97	0.17	0.008	7.22	11.15	2.40	0.44	0.23		
Hualalai	51.49	2.28	14.09	0.10	10.49	0.16	0.008	7.53	11.39	2.30	0.37	0.22		
Haleakala	51.76	2.38	13.47	0.10	10.87	0.17	0.008	7.84	11.11	1.96	0.36	0.26		
4b.	SiO ₂	TiO ₂	Al ₂ O ₃	Cr ₂ O ₃	FeO	MnO	NiO	MgO	CaO	Na ₂ O	K ₂ O	P ₂ O ₅	Final olivine	Average olivine
Mauna Kea Low SiO ₂	46.76	1.97	10.47	0.21	11.78	0.17	0.080	17.71	8.59	1.79	0.31	0.16	90.5	86.7
Mauna Kea High SiO ₂	48.25	1.83	10.06	0.21	11.72	0.17	0.090	17.72	7.88	1.64	0.28	0.15	90.5	86.4
Mauna Loa	49.13	1.59	10.52	0.20	10.60	0.16	0.080	17.37	8.29	1.67	0.24	0.14	91.2	87.7
Ko'olau	48.70	1.76	10.67	0.21	11.34	0.17	0.091	17.14	7.85	1.63	0.29	0.16	90.5	86.5
Kilauea	48.13	1.83	10.05	0.21	11.38	0.17	0.095	17.58	8.29	1.77	0.32	0.17	90.7	86.7
Hualalai	48.31	1.69	10.48	0.21	10.78	0.16	0.087	17.68	8.47	1.70	0.27	0.16	91.2	87.5
Haleakala	48.45	1.78	10.08	0.21	11.22	0.17	0.075	17.48	8.64	1.46	0.27	0.19	90.5	86.7
4c.	SiO ₂	TiO ₂	Al ₂ O ₃	Cr ₂ O ₃	FeO	MnO	NiO	MgO	CaO	Na ₂ O	K ₂ O	P ₂ O ₅	Final olivine	Average olivine
Mauna Kea Low SiO ₂ glass	48.46	2.55	13.63	0.10	11.74	0.17	0.008	8.76	11.06	2.37	0.37	0.20		
Mauna Kea High SiO ₂ glass	51.19	2.32	13.01	0.10	10.48	0.17	0.008	8.47	11.09	2.11	0.36	0.19		
Mauna Kea Low SiO ₂	46.31	1.87	10.04	0.22	11.75	0.16	0.072	19.27	8.15	1.73	0.27	0.15	91.2	88.0
Mauna Kea High SiO ₂	48.69	1.78	10.02	0.20	10.75	0.17	0.062	17.75	8.55	1.61	0.27	0.15	91.2	87.7

4d.	SiO ₂	TiO ₂	Al ₂ O ₃	Fe ₂ O ₃ *	MnO	MgO	CaO	Na ₂ O	K ₂ O	P ₂ O ₅
KSDP	47.17	1.96	12.23	10.95	0.16	8.47	9.25	2.13	0.29	0.20
Mauna Kea - HSDP2	47.95	2.19	11.14	12.67	0.18	14.06	9.35	1.77	0.26	0.22
SOH-1	49.99	2.58	13.31	12.54	0.16	7.62	10.36	2.19	0.43	0.27
Mauna Loa -HSDP2	49.21	1.80	11.72	12.35	0.17	13.56	9.06	1.65	0.22	0.18

Table 4: Results of glass composition compilation, olivine addition, and compositional averaging calculations presented in this study.

Table 4a shows the starting liquid compositions calculated by averaging measured glass compositions from sources as described in the text. NiO and Cr₂O₃ contents are typically not measured in glasses and so were assumed here. Table 4b gives the calculated liquid composition at the end of the olivine addition calculations. The final olivine composition gives the Mg # composition of the final olivine added to the liquid, and the average olivine composition is the mass-weighted average Mg# of olivine added during the analysis. Table 4c shows the alternate calculations referred to in the text; the lava series from Mauna Kea were fit using a more magnesian liquid and ended at a more forsteritic olivine composition to try to better fit the olivine composition seen in the regression and histogram analyses. Table 4d gives the average weighted composition for the KSDP drill core through Ko'olau, the HSDP2 sections for Mauna Kea and Mauna Loa, and the SOH-1 drill core through Kilauea.

Table 5

Volcano/section	Percent of mass left behind	Source
Kilauea	10-22%	Clague & Denlinger, 1994
Mauna Kea	4-7%	Baker et al., 1996
Mauna Loa	7.8%	HSDP2
Mauna Loa	16.7%	Historic
Kilauea	18.9%	Historic and Pu'u O'o
Kilauea	20.5%	SOH-1
Mauna Kea	6.7%	HSDP2
Ko'olau	17.8%	KSDP
Mauna Kea high MgO section	0.5%	HSDP2
Mauna Kea Low MgO section	12.7%	HSDP2
Mauna Kea high MgO liquid	9.0%	HSDP2

Table 5: The percent of mass of the liquid entering each volcano that is deposited within the volcano as accumulated olivine based on the data sets examined here. The high and low MgO sections for Mauna Kea in the HSDP2 drill core are as defined in the text. The high MgO liquid value is the value for the full core using the high MgO liquid for Mauna Kea from Table 4c.

FIGURE CAPTIONS

Fig 1. Compilation of point count data for available drill cores and other selected data sets. Line is best fit line for counts from HSDP2 – this work. All data is plotted as whole rock wt% MgO versus olivine modal abundance measured by point counts on the same unit. All olivine modal abundances are normalized to a vesicle-free basis in this case.

Figure 2. Whole rock FeO* versus MgO (wt. %) for tholeiites from the eight best-sampled Hawaiian volcanoes. All iron is taken as FeO*, as in the text. Solid lines represent linear regression best fit lines for the data and represent the average olivine control line for each volcano. Dashed curves reflect 95% confidence limits for the olivine control regression lines. Numbers of points plotted for each volcano are as listed in Table 1 and sources are given in Supplementary Table 1.

Figure 3. Histogram of whole rock wt. % FeO* contents from Mauna Kea and Ko'olau. The median value for Ko'olau is 10.6, while Mauna Kea is 11.3.

Figure 4. Whole rock analyses from the HSDP2 drill core, divided into low and high SiO₂ series based on the measurements of Stolper et al. (2004).

Figure 5. Histograms of olivine populations from the best-sampled Hawaiian volcanoes.

Figure 6. Whole rock wt. % MgO variations from the four volcanoes sampled by the major drill cores analyzed in this project. Ages are calculated as described in the text.

Solid lines are five point unweighted moving averages calculated for each volcano.

Decreasing or increasing the number of points included in the moving average typically only increases or decreases, respectively, the magnitude of the shifts but does not change the overall structure. For each core, units that were sampled more than one time were averaged to produce a single result for each sampled unit, and that result is plotted here.

Data for Mauna Kea cover a number of different flow types and therefore were separated by flow type here, although the moving average is calculated across each flow type.

Figure 7. Whole rock wt. % MgO variations measured from historically dated eruptions from Mauna Loa and Kilauea. No samples are included in this plot from the long-lived Pu'u O'o eruption phase from Kilauea. Several points along a horizontal line are typically measurements of different samples from a single eruption. The 1959 eruption of Kilauea produced a lava lake that was sampled over a number of years as it cooled and crystallized, and thus samples from it represent variable amounts of olivine accumulation, loss, and crystallization of other phases. Data sources are given in Supplemental Table 1.

Figure 8. Dated whole rock sample measurements from the long-lived Pu'u O'o eruption phase at Kilauea. Data sources are given in Supplemental Table 1.

Figure 9. CaO contents in olivines measured by Sobolev et al. (2007). Only analyses from this study were considered so that the analytical conditions in each measurement would remain constant. Red line in panel Mauna Kea shows the estimated increase in olivine CaO content predicted during olivine crystallization by the model of Libourel

(1999). Samples move to lower CaO contents by re-equilibration with a high MgO, low CaO liquid, likely while residing in a cumulate pile. A few samples from Loihi show noticeably lower values, likely reflecting equilibration with a low CaO liquid that has previously crystallized plagioclase.

Figure 10. weight fraction of olivine crystallized by Mg # during the olivine addition calculations. Totals were calculated by summing the weight crystallized during every 0.5 Mg# units and normalizing by the total amount of olivine crystallized between the primary liquid and the end of the calculation at 7.4% MgO. This calculation was done specifically for the high SiO₂ series from Mauna Kea, but a similar trend could be calculated for any volcano. The large peaks in Mg# seen in the histograms (Figure 5) and the Mg# at which this peak occurs are not predicted by this calculation without re-equilibration.

Figure 11. Whole rock Al₂O₃ and CaO contents as calculated in the olivine addition analyses. The blue line segment shows the actual whole rock compositions calculated by olivine addition. The solid line at lower CaO content is the extension of this addition trend back to zero Al₂O₃ content. The higher line shows the increase in projected CaO content if 0.2% CaO is added to the high Mg, low CaO and Al₂O₃ liquid, proposed here to be sourced from the decreasing CaO content in re-equilibrating olivines.

Figure 12. Histogram of measured NiO concentrations in olivines from Mauna Kea, as measured by Sobolev et al., (2007). The median measured NiO concentration is .379. As

in Figure 10 with MgO, the olivine addition calculations predict a fairly uniform distribution of NiO contents as crystallization proceeds. The large peak in number of olivines measured close to the average NiO content suggests many of these olivines have re-equilibrated towards the average composition while inside the volcano.

FIGURES

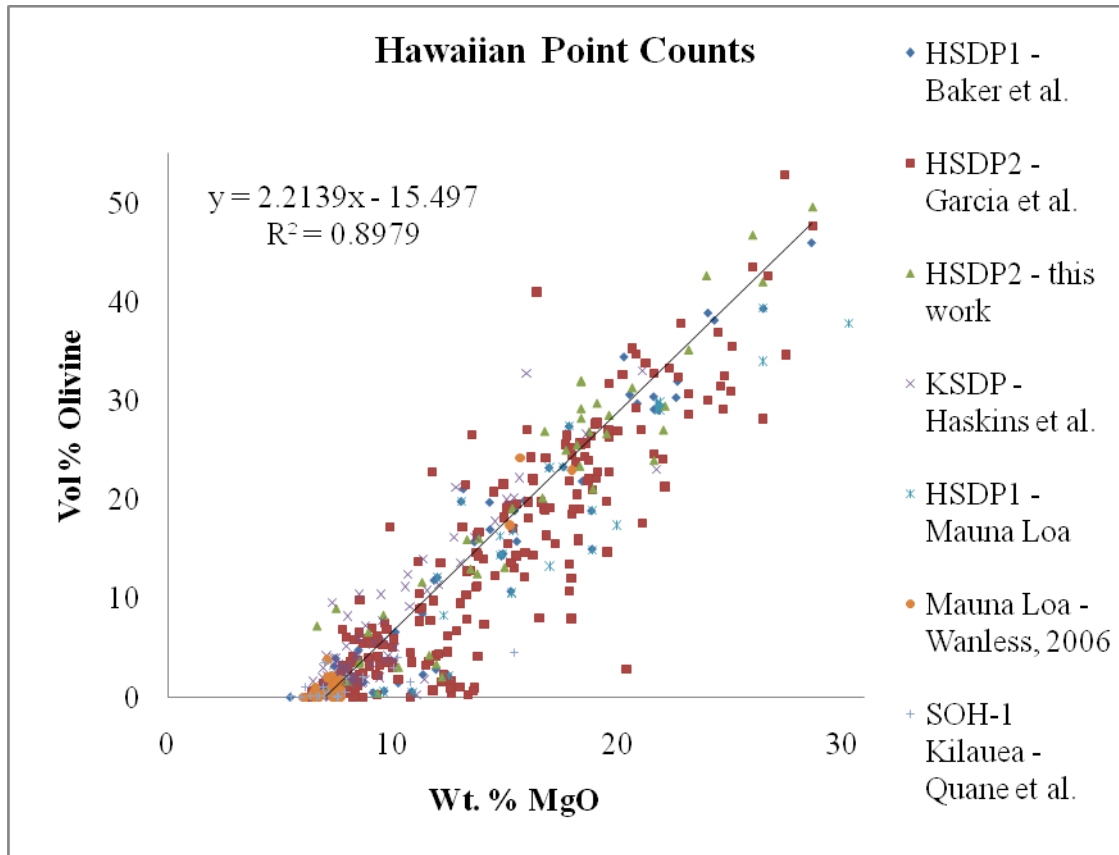


Figure 1

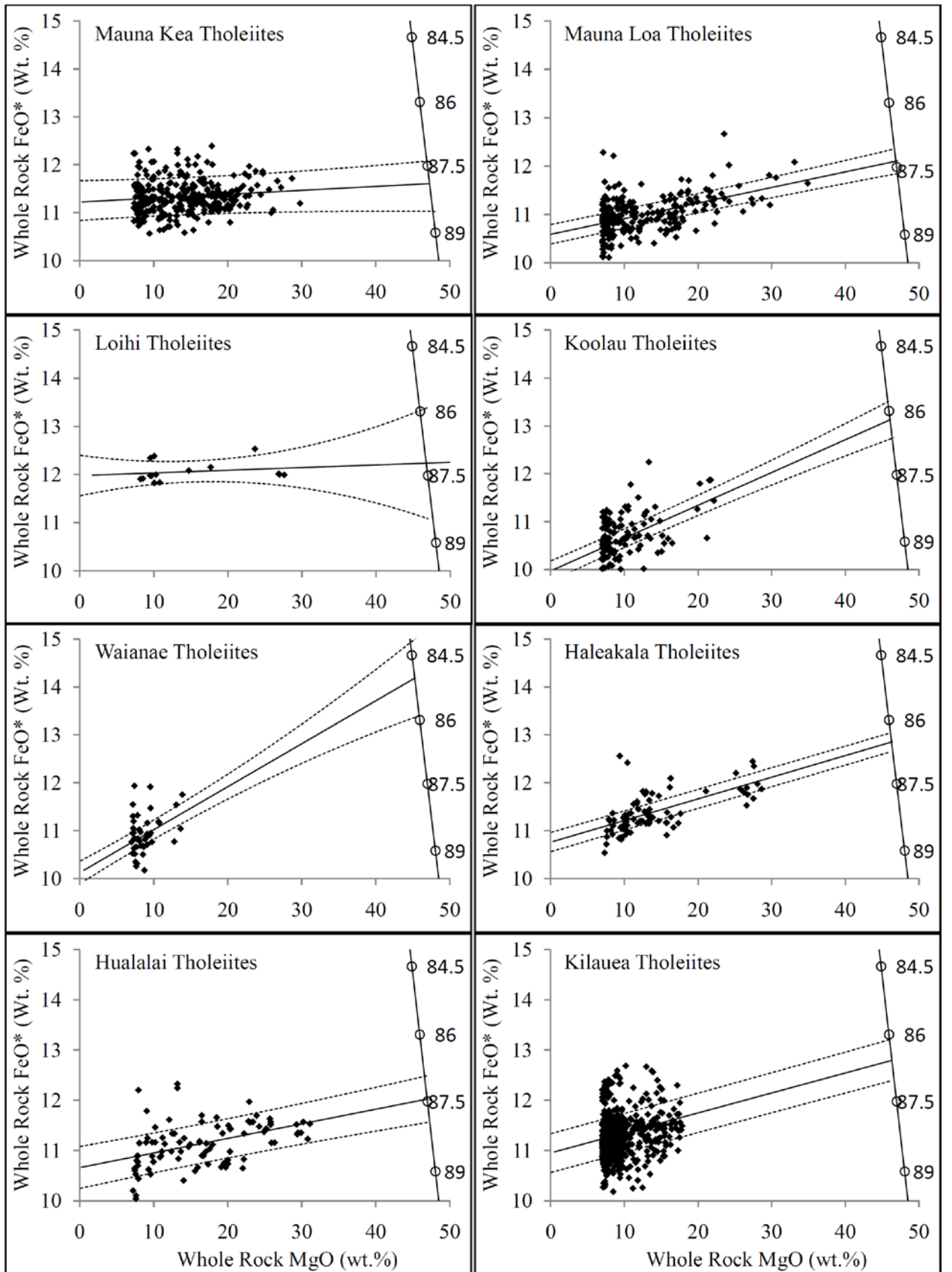


Figure 2

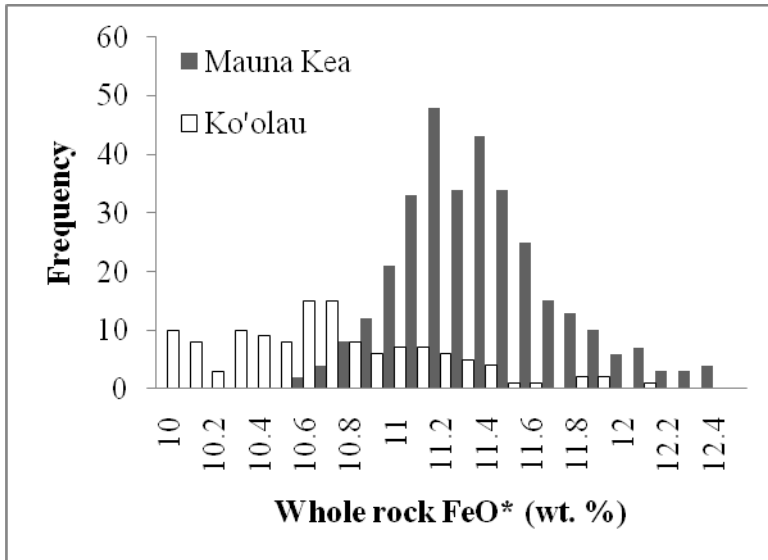


Figure 3

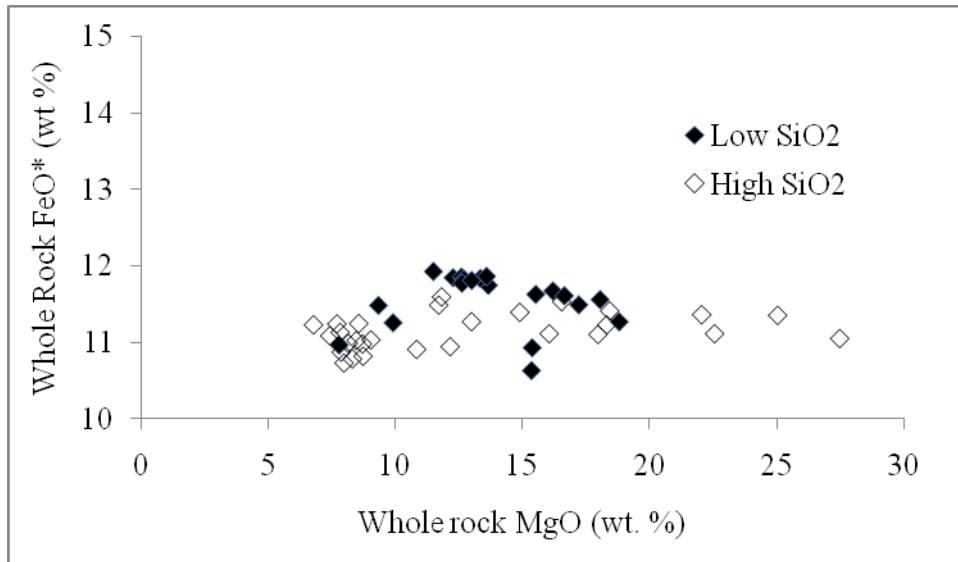


Figure 4

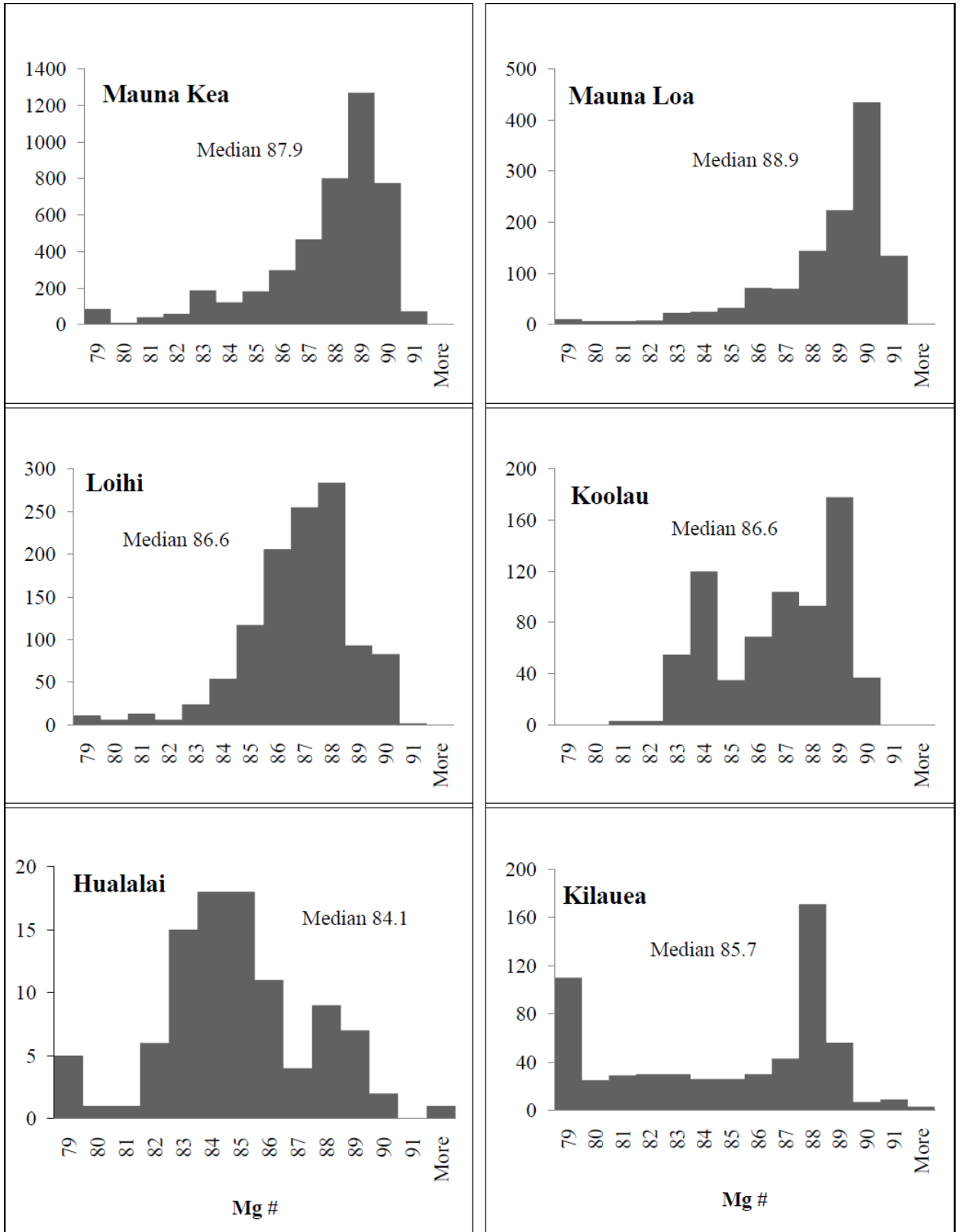


Figure 5

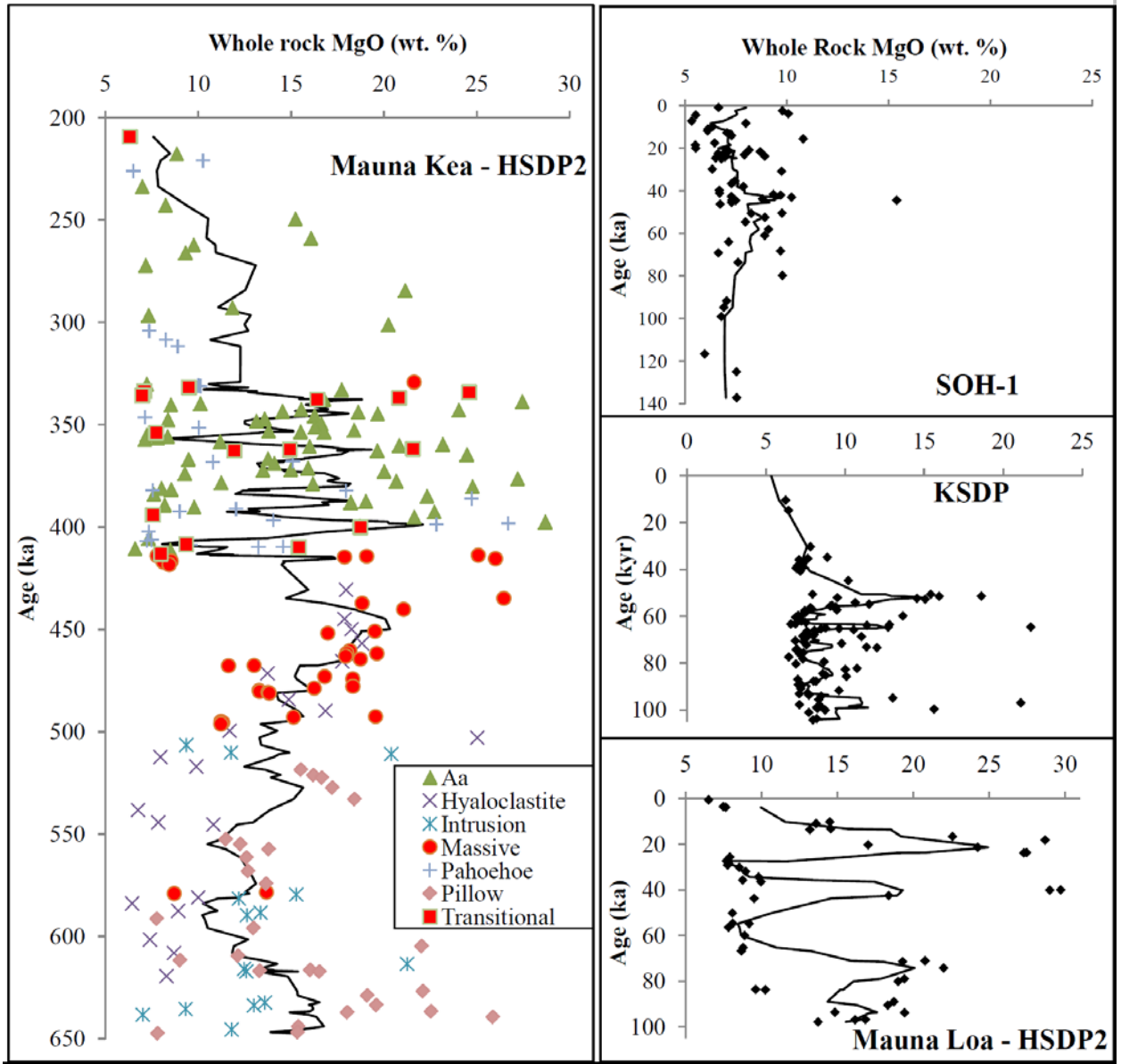


Figure 6

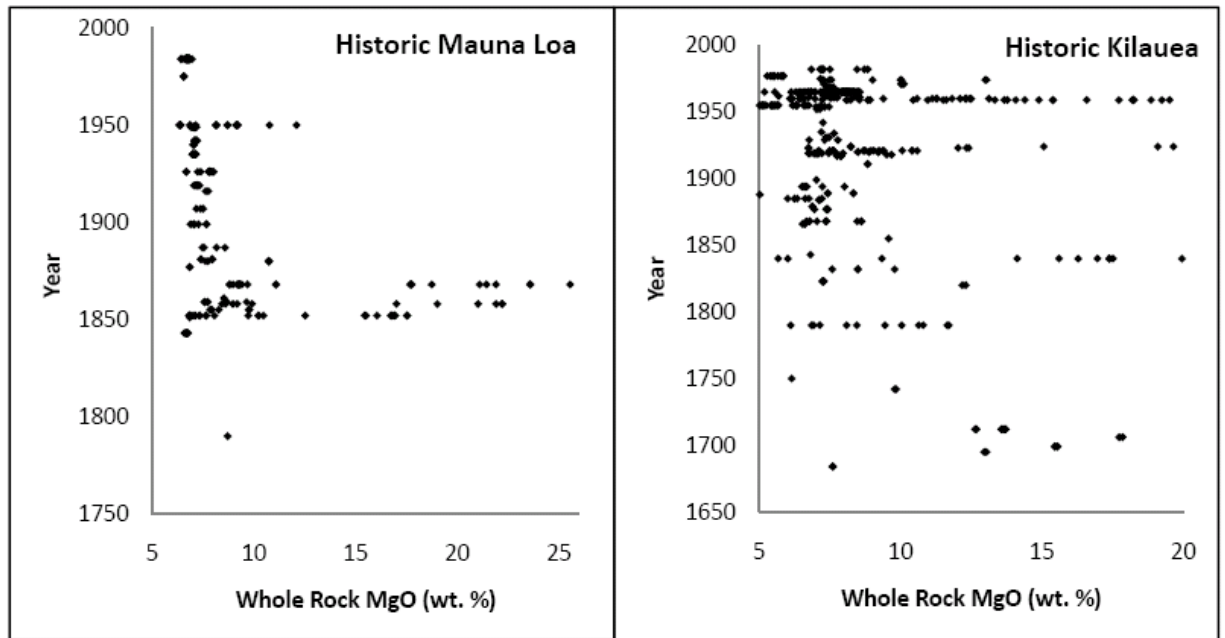


Figure 7

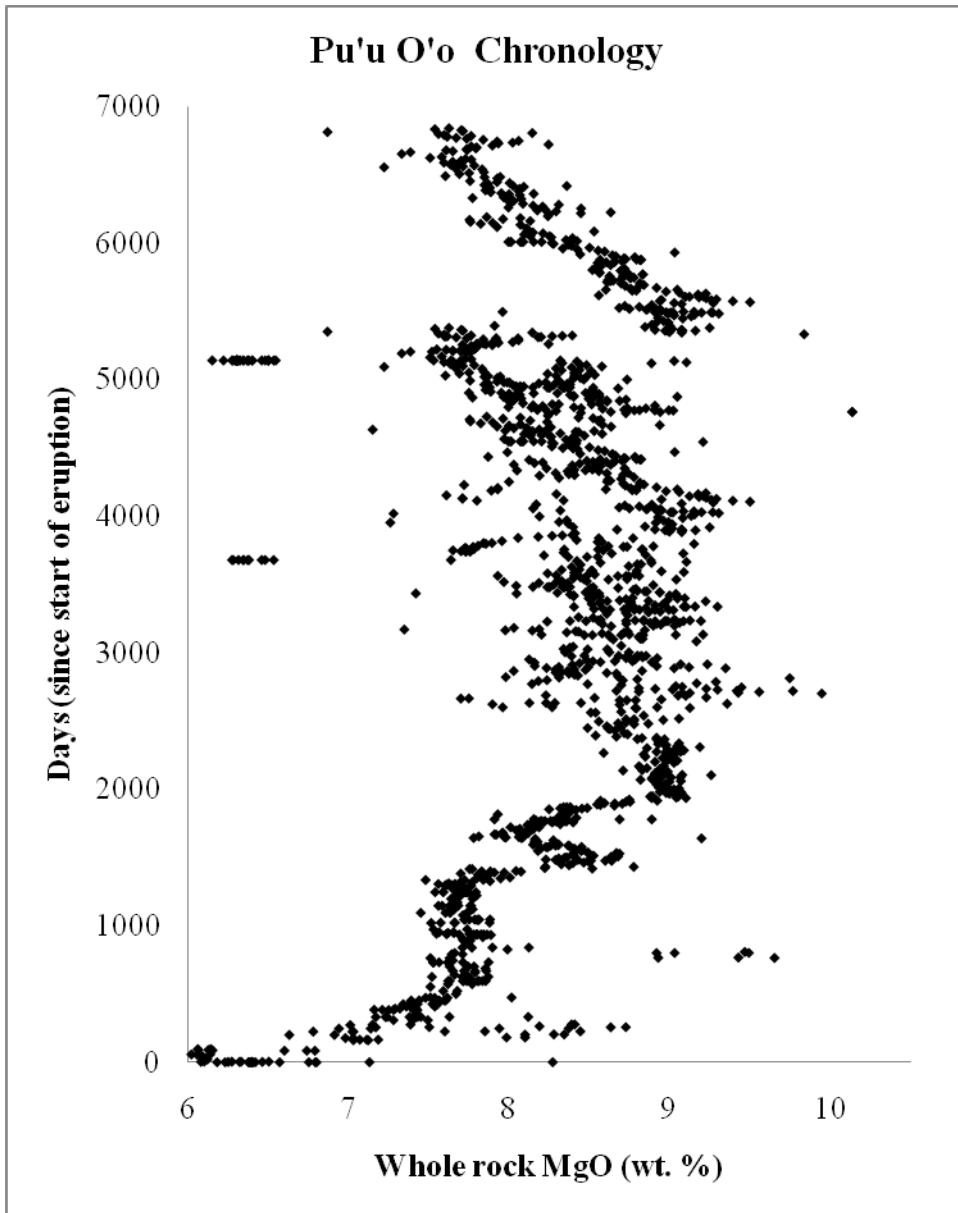


Figure 8

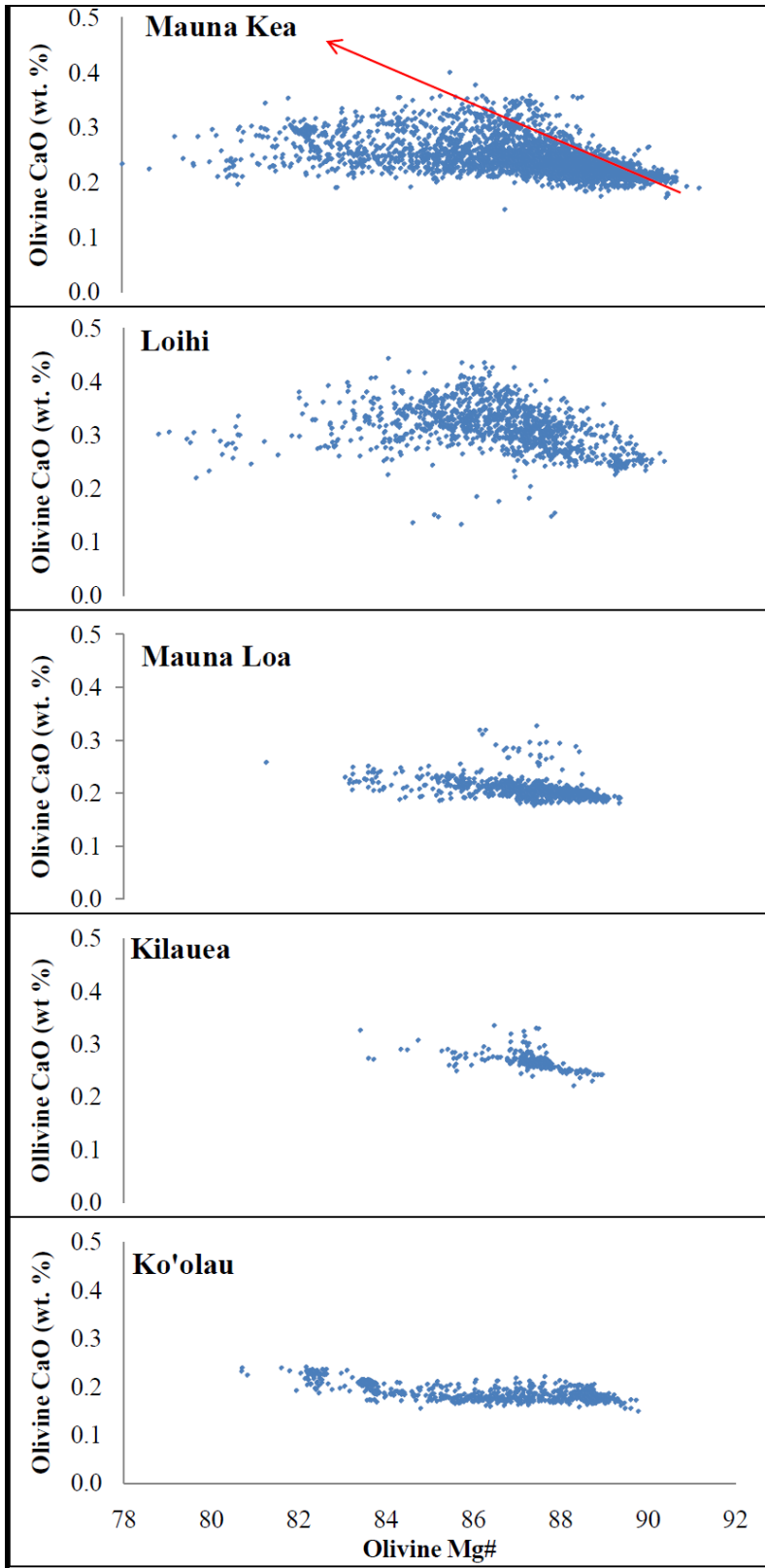


Figure 9

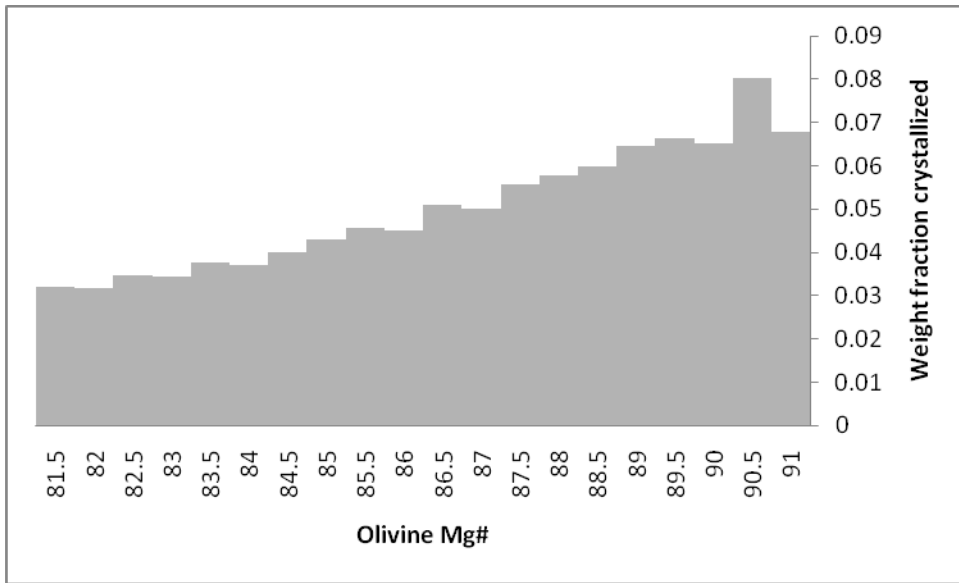


Figure 10

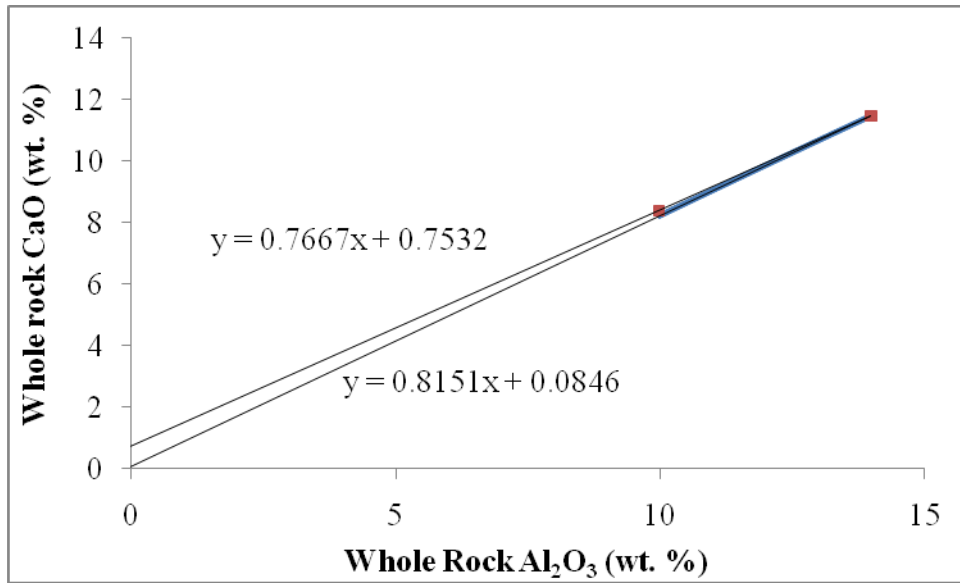


Figure 11

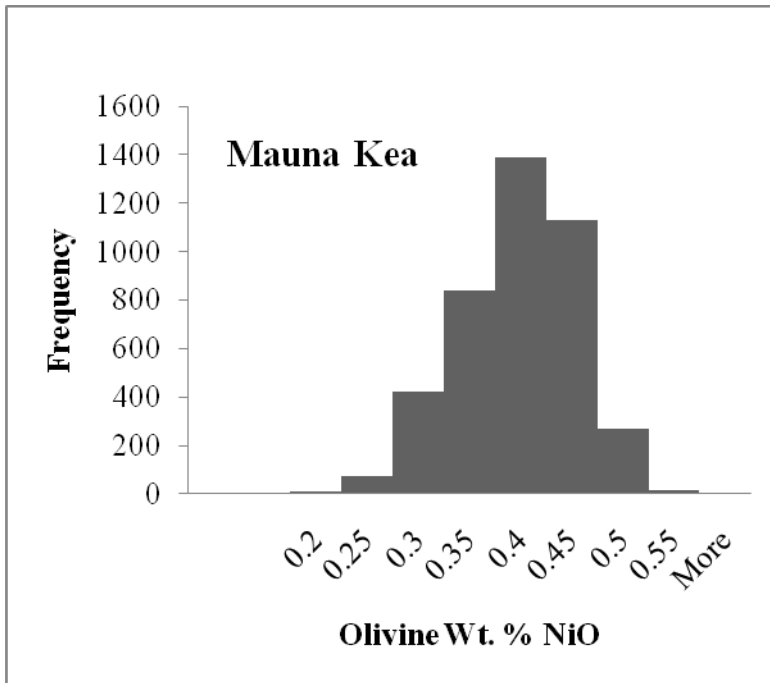


Figure 12: